ORIGINAL ARTICLE

Journal of Cachexia, Sarcopenia and Muscle 2019; **10**: 391–410
Published online 30 January 2019 in Wiley Online Library (wileyonlinelibrary.com) **DOI:** 10.1002/jcsm.12374

LncIRS1 controls muscle atrophy via sponging miR-15 family to activate IGF1-PI3K/AKT pathway

Zhenhui Li[1,2], Bolin Cai[1,2], Bahareldin Ali Abdalla[1,2], Xuenong Zhu[1,2,3], Ming Zheng[1,2], Peigong Han[1,2], Qinghua Nie[1,2]* & Xiquan Zhang[1,2]

[1]*Department of Animal Genetics, Breeding and Reproduction, College of Animal Science, South China Agricultural University, Guangzhou 510642, Guangdong, China,* [2]*Guangdong Provincial Key Lab of Agro-Animal Genomics and Molecular Breeding, and Key Laboratory of Chicken Genetics, Breeding and Reproduction, Ministry of Agriculture, Guangzhou, Guangdong, China,* [3]*Institute of Biotechnology, Nanchang Normal University, Nanchang 330032, Jiangxi, China*

Abstract

Background Recent studies indicate important roles for long noncoding RNAs (lncRNAs) in the regulation of gene expression by acting as competing endogenous RNAs (ceRNAs). However, the specific role of lncRNAs in skeletal muscle atrophy is still unclear. Our study aimed to identify the function of lncRNAs that control skeletal muscle myogenesis and atrophy.

Methods RNA sequencing was performed to identify the skeletal muscle transcriptome (lncRNA and messenger RNA) between hypertrophic broilers and leaner broilers. To study the 'sponge' function of lncRNA, we constructed a lncRNA-microRNA (miRNA)-gene interaction network by integrated our previous submitted skeletal muscle miRNA sequencing data. The primary myoblast cells and animal model were used to assess the biological function of the *lncIRS1 in vitro* or *in vivo*.

Results We constructed a myogenesis-associated lncRNA-miRNA-gene network and identified a novel ceRNA lncRNA named *lncIRS1* that is specifically enriched in skeletal muscle. *LncIRS1* could regulate myoblast proliferation and differentiation *in vitro*, and muscle mass and mean muscle fibre *in vivo*. *LncIRS1* increases gradually during myogenic differentiation. Mechanistically, *lncIRS1* acts as a ceRNA for miR-15a, miR-15b-5p, and miR-15c-5p to regulate *IRS1* expression, which is the downstream of the *IGF1* receptor. Overexpression of *lncIRS1* not only increased the protein abundance of *IRS1* but also promoted phosphorylation level of AKT (p-AKT) a central component of insulin-like growth factor-1 pathway. Furthermore, *lncIRS1* regulates the expression of atrophy-related genes and can rescue muscle atrophy.

Conclusions The newly identified *lncIRS1* acts as a sponge for miR-15 family to regulate *IRS1* expression, resulting in promoting skeletal muscle myogenesis and controlling atrophy.

Keywords Atrophy; ceRNA; *IRS1*; Myogenesis; lncRNA-miRNA-gene network

Received: 23 July 2018; Accepted: 12 November 2018
**Correspondence to: Qinghua Nie, Department of Animal Genetics, Breeding and Reproduction, College of Animal Science, South China Agricultural University, Guangzhou 510642, Guangdong, China. Tel: 86-20-85285759, Fax: 86-20-85280740, Email: nqinghua@scau.edu.cn*

Abbreviations

miRNA – microRNA
lncRNAs – long noncoding RNAs
CCK-8 – cell counting kit-8
NC – negative control
ceRNA – competing endogenous RNA
MREs – miRNA response elements
IPA – ingenuity pathway analysis
EdU – 5-ethynyl-2′-deoxyuridine

Introduction

A decrease in adult muscle mass and fibre size is called 'atrophy' and is characterized by enhanced protein degradation.[1–3] An increase in muscle mass, called 'hypertrophy', is associated with increased protein synthesis.[3] Therefore, the maintenance of muscle mass is controlled through a balance between protein synthesis and protein degradation

pathways.[1] Skeletal muscle atrophy occurs in a variety of conditions, such as cancer cachexia, prolonged periods of muscle inactivity, and aging itself. Unfortunately, there are no effective pharmacological treatments for this devastating disease.

Skeletal muscle myogenesis and hypertrophy is a multistep process that comprises four major stages: in the initial stage, muscle precursor cells differentiate from the somite; in the second stage, myogenic precursor proliferation and differentiation gives rise to myoblasts; in the third stage, myoblast differentiation gives rise to myotubes; and finally, myofibers are formed from the myotubes.[4] These complex cellular and development processes depend on the precise spatiotemporal expression of regulatory factors. Insulin receptor substrate 1 (*IRS1*) is a signalling adapter protein, essential for skeletal muscle growth and protein homeostasis. Mice lacking *IRS1* have reduced growth rate by 40–70% compared to controls.[5,6] *IRS1* plays a key role in transmitting signals from the insulin and insulin-like growth factor-1 (IGF-1) receptors to intracellular signalling pathway PI3K/AKT. IGF1-PI3K/AKT pathway is a key intracellular signalling mechanism controlling muscle hypertrophy.[7] In addition, evidence suggests that in complex organism development, RNA contains a hidden layer of regulatory information. It not only functions as a messenger between DNA and the protein but also plays a role in the modulation of gene expression.[8] Long noncoding RNAs (lncRNAs), a novel class of regulatory RNAs, commonly defined as transcribed RNAs with sizes ranging from 200 bp to $>$100 kb, are involved in numerous important biological processes.[9,10] For example, *SRA*, a lncRNA, was demonstrated to facilitate myoblast differentiation by controlling the transcriptional activity of *MyoD*.[11] Salmena[12] previously presented a competing endogenous RNA (ceRNA) hypothesis that was supported by many evidences.[13,14] LncRNAs can function as ceRNAs protect messenger RNAs (mRNAs) by acting as molecular sponges for microRNAs (miRNAs) that specifically inhibit the target mRNAs (Figure S1). For example, *Linc-MD1* acts as a ceRNA by sponging miR-133 and miR-135 to regulate the expression of *MAML1* and *MEF2C*, which are transcription factors that activate late-differentiation muscle genes.[15] In addition, lncRNA *H19*, which is highly expressed in the developing embryo and in adult muscle, functions as a molecular sponge for the let-7 family and thereby regulates muscle differentiation.[16] Although functions of these lncRNAs have been partially characterized, most of their roles for myogenesis and anti-atrophy are still poorly understand. Therefore, the aim of our study is to explore the role of lncRNAs in regulating of skeletal muscle myogenesis and anti-atrophy.

In this study, we first focused on skeletal muscle myogenesis associated-lncRNAs and constructed a ceRNA network (lncRNA-miRNA-gene network) *in silico*. We investigated the function of a novel lncRNA named *lncIRS1* in skeletal muscle myogenesis. *LncIRS1* was highly expressed in skeletal muscle and promoted proliferation and differentiation of myoblast. Mechanistic investigations showed that *lncIRS1* functioned as a ceRNA by sponging miR-15a, miR-15b-5p, and miR-15c-5p, which then activated *IRS1* and regulated the IGF-1 signalling pathway, a critical pathway of skeletal muscle myogenesis. Moreover, the effect of *lncIRS1* overexpression and knockdown on skeletal muscle atrophy induced by dexamethasone was investigated. Our study provides some clues regarding *lncIRS1* mechanism of regulation in skeletal muscle myogenesis and atrophy.

Material and methods

Animals

Seven-week-old of hypertrophic (WRR) and leaner broilers (XH) were used. All human and animal studies have been approved by the appropriate ethics committee and have therefore been performed in accordance with the ethical standards laid down in the 1964 Declaration of Helsinki and its later amendments.

RNA sequencing (RNA-Seq)

Breast muscle tissues from WRR and XH broilers were used for RNA-seq. Total RNA was isolated using Trizol Reagent (Invitrogen, Carlsbad, CA, USA) according to the manufacturer's protocol. RNA quantity and quality were evaluated on an Agilent 2100 Bioanalyzer (Agilent technologies, Waldbronn, Germany), and RNA integrity was further examined using agarose gel electrophoresis. Ribosomal RNA (rRNA) was removed from the total RNA using Epicentre Ribo-ZeroTM rRNA Removal Kit (Epicentre, Madison, Wisconsin, USA) following the manufacturer's instructions. Subsequently, the RNA from four broilers within each group was mixed in equal amounts to construct a pooled sample for each group. High-throughput RNA-seq was performed on the Illumina Hiseq 2000 platform (Illumina, San Diego, CA, USA). The raw Illumina sequencing reads were cleaned by removing empty reads, adapter sequences, reads with over 10% N sequence, and low-quality reads in which the number of bases with a quality value Q $\leq$ 10 was greater than 50%. In addition, rRNA reads were identified by blasting against the rRNA database (http://www.arb-silva.de/) using SOAP software and removed from the dataset. The filtered reads were mapped to the chicken reference genome (ftp://ftp.ensembl.org/pub/release-73/fasta/gallus_gallus/dna/) using Tophat2. The mapped reads were assembled and transcripts were constructed using Cufflinks 2.0.2. The Ensembl, NCBI RefGene, and UCSC databases were chosen as annotation references for lncRNA analyses. RNA length $\geq$ 200 nt, CPC score $\leq$ 0, CPAT probability $\leq$ 0.364, and phyloCSF score ≤ -20 were used to evaluate the coding potential of transcripts. The RefSeq and Ensembl databases were used for gene analysis.

The expression levels of the transcripts are expressed as fragments per kilobase of transcript per million mapped reads values. Differentially expressed transcripts for were identified using Cuffdiff, using q-value <0.001 and $|(\text{fold change})| \geq 2$ as the cut-off. The sequencing data obtained from the RNA-Seq were released to the GEO database under accession number GSE58755.

Construction of lncRNA-miRNA-gene interaction network

Previous study proposed a ceRNA hypothesis that protein-coding RNAs and lncRNAs containing the common one or more miRNA response elements (MREs) can compete for binding to miRNAs and regulate each other's expression.[12] To study the 'sponge' function of lncRNA, we constructed a lncRNA-miRNA-gene interaction network by integrated our previous submitted skeletal muscle miRNA sequencing data (GSE62971). The lncRNA-miRNA-gene crosstalk network construction involved the following three components: (i) interactions between miRNAs and genes, (ii) interactions between lncRNAs and miRNAs, and (iii) interaction between genes and genes. Firstly, the potential target genes of differentially expressed miRNAs were predicted with TargetScan; miRNAs repress their target genes expression at post-transcriptional level. Therefore, the predicted target genes that have an opposition expression patterns of their corresponding miRNAs were selected as candidate targets for differentially expressed miRNAs. Secondly, RNAhybrid, a tool for finding the minimum free energy hybridization of a long and a short RNA, was used to predict the target lncRNA of differentially expressed miRNA. As miRNA can repress the expression of mRNA, it also can inhibit the expression of its target lncRNAs. Therefore, the predicted target lncRNAs that have an opposition expression patterns of their corresponding miRNAs were selected as candidate target lncRNAs for differentially expressed miRNAs. Thirdly, ingenuity pathway analysis (IPA), a database of known and predicted protein interactions, was used to construct gene–gene interactions. Finally, lncRNA-miRNA-mRNA interaction network was constructed using Cytoscape. The Molecule Annotation System 3.0 (http://bioinfo.capitalbio.com/mas3) was used to identify GO terms and pathways enriched in genes belonging to lncRNA-miRNA-gene interaction network.

In situ hybridization

Whole-mount *in situ* hybridization of chick embryos was performed according to a standard *in situ* hybridization protocol.[17] Digoxigenin-labelled probes were synthesized to detect *IRS1* and *lncIRS1*. *IRS1*: Forward: ACCTGGACTTGGTG AAGGATTGC; Reverse: AATTAACCCTCACTAAAGGGA GACCCA TTTACAGAGGAAGAGGAGGAG. *LncIRS1*: Forward: GTATTG GTCA CTCTGGGTCAG; Reverse: AATTAACCCTCACTAAAGGGA GATCTTCACTTT CTCCTTGGGTA. The whole embryos at stage HH10 were fixed with 4% paraformaldehyde overnight at 4°C, dehydrated in a graded series of methanol, and stored at −20°C (overnight). Next, the embryos were hybridized with *IRS1* or *lncIRS1* digoxigenin-labelled probe overnight at 65°C. After hybridization, the bound RNA probe was visualized by incubation with alkaline phosphatase-conjugated anti-digoxigenin antibodies, and the colour was developed in NBT/BCIP (Roche, Basel, Switzerland). The whole-mount stained embryos were photographed under a stereomicroscope (Olympus MVX10).

Cell culture, treatment, and transfection

Chicken embryonic fibroblast cell line (DF-1 cells) were cultivated with Dulbecco's modified Eagle's medium (Gibco, Grand Island, NY, USA) supplemented with 10% foetal bovine serum (Gibco) and 0.2% penicillin/streptomycin (Gibco) in a humidified atmosphere with 5% (v/v) CO_2 at 37°C.

Chicken primary myoblasts were isolated from E11 chicken leg muscles as previously described.[18] Chicken primary myoblasts were cultured with growth medium consisting of RPMI-1640 medium (Gibco), 20% foetal bovine serum, and 0.2% penicillin/streptomycin. After myoblasts achieving 100% cell confluence, the growth medium was then removed and replaced with differentiation medium (RPMI-1640 medium, 2% horse serum and 0.2% penicillin/streptomycin). For cell treatments, myotubes were treated with vehicle and 10 μM dexamethasone (Sigma-Aldrich, St. Louis, Mo, USA) in RPMI-1640 for 24 h. All transient transfections were performed with Lipofectamine 3000 reagent (Invitrogen, USA) according to manufacturer's direction.

RNA extraction, complementary DNA (cDNA) synthesis, and quantitative real-time PCR (qRT-PCR)

Total RNA was extracted from tissues or cells using TRIzol reagent (Invitrogen Life Technologies, Carlsbad, CA, USA) as recommended by the supplier. A PARIS Kit (Ambion, Life Technologies, USA) was used to harvest the cytoplasmic and nuclear cell lysates of myoblast, following the manufacturer's protocol; cDNA synthesis for RNA (mRNA and lncRNA) was carried out using the PrimeScript RT Reagent Kit with gDNA Eraser (Perfect Real Time) (TaKaRa, Otsu, Japan). For miRNA, bulge-Loop™ miRNA qRT-PCR primers specific for miR-15 family and U6 were designed by RiboBio (RiboBio, Guangzhou, China), and ReverTra Ace qPCR RT Kit (Toyobo, Osaka, Japan) was used to synthesize cDNA. Real-time quantitative PCR (qPCR) reactions were performed on

a Bio-Rad CFX96 Real-Time Detection System using iTaq Universal SYBR Green Supermix Kit (Bio-Rad Laboratories Inc., USA). Data analyses were performed using the $2^{-\Delta\Delta Ct}$ method as described previously.[19] Chicken *β-actin* and *U6* were used as internal controls.

RNA oligonucleotides and plasmids construction

The gga-miR-15 family mimics (miR-15a, miR-15b-5p, miR-15c-5p, miR-16-5p, and miR-16c-5p), mimic negative control, siRNA target against the *IRS1* gene (si-IRS1), siRNA target against the *lncIRS1* gene (si-lncIRS1), and siRNA nonspecific control were designed and synthesized by RiboBio (Guangzhou, China).

The *IRS1* overexpression construct was generated by amplifying the *IRS1* coding sequence, which subsequently integrated into the HindIII/KpnI restriction sites of the pcDNA3.1 overexpression plasmid (named pcDNA3.1-IRS1). The full-length sequence of *lncIRS1* was subcloned into the BamHI/XhoI restriction sites of the pcDNA3.1 overexpression plasmid (named pcDNA3.1-lncIRS1). The empty pcDNA3.1 vector was used as control plasmid.

MiR-15 family binding sites in *IRS1* 3'UTR or *lncIRS1* (three binding sites: Site 1 at position 2651–2657 of *lncIRS1*; Site 2 at position 3438–3444 of *lncIRS1*; and Site 3 at position 3775–3781 of *lncIRS1*) were amplified by PCR using a cDNA template synthesized from total RNA. Then, the PCR products were subcloned into XhoI/XbaI restriction sites in the pmirGLO dual-luciferase reporter vector to generate the pmirGLO-IRS1 reporter, pmirGLO-site 1 of *lncIRS1* reporter, pmirGLO-site 2 of *lncIRS1* reporter, and pmirGLO-site 3 of *lncIRS1* reporter.

For identification of the coding ability of *lncIRS1*, seven possible Open Reading Frames (ORFs) of *lncIRS1* were amplified and cloned into pSDS-20218 vector (SiDanSai, Shanghai, China). Chicken *β-actin* gene was subcloned into pSDS-20218 vector as positive control.

5′ and 3′ rapid amplification of cDNA ends (RACE)

A SMARTer RACE cDNA Amplification Kit (Clontech, Osaka, Japan) was used to obtain the full-length sequences of *lncIRS1* and *IRS1*, following the manufacturer's instructions. Nested-PCR reactions were performed. The products of the RACE PCR were cloned into the pJET 1.2/blunt cloning vector (CloneJET PCR Cloning Kit; Fermentas, Glen Burnie, MD, USA) and sequenced by Sangon Biotech (Shanghai, China).

Dual-luciferase reporter assay and RNA immunoprecipitation

DF-1 cells were seeded in 96-well plates 1 day before transfection and then co-transfected with (I) pmirGLO-IRS1 reporter, (II) pmirGLO-site 1 of *lncIRS1* reporter, (III) pmirGLO-site 2 of *lncIRS1* reporter, and (IV) pmirGLO-site 3 of *lncIRS1* reporter, and miRNA mimics or mimic NC using Lipofectamine 3000 reagent. After 48 h, luciferase activity analysis was performed using a Fluorescence/Multi-Detection Microplate Reader (BioTek, Winooski, VT, USA) and a Dual-GLO Luciferase Assay System Kit (Promega, USA). The firefly luciferase activities were normalized to Renilla luminescence in each cell-well.

RNA immunoprecipitation used the Magna RIP RNA-Binding Protein Immunoprecipitation Kit (Millipore, Billerica, MA, USA) and the anti-Argonaute2 (AGO2) antibody (Abcam, Cambridge, UK) according to the manufacture's protocol. After the antibody was recovered by protein A + G beads, qRT-PCR was performed to detect *IRS1*, *lncIRS1*, and miR-15 family in the precipitates.

Western blotting

Myoblast cells were seeded in six-well plates and transfected with overexpression plasmid, siRNA, or miRNA mimics for 48 h. Cells and muscle tissue were harvested, washed with 1× phosphate buffered saline (PBS) and lysed in RIPA lysis buffer. Immunoblotting was performed using standard procedures and various antibodies. The primary antibodies used were anti-IRS1 (1:1000; catalogue no. ab5603, Abcam, Cambridge, UK), anti-phospho-AKT (1:1000; catalogue no. #4040, Cell Signaling Technology, Danvers, MA, USA), anti-AKT (1:1000; catalogue no. #9272, Cell Signaling Technology), anti-MyHC (1:50; catalogue no. B103, Developmental Studies Hybridoma Bank, Iowa City, Iowa, USA), anti-MyoG (1:1000; catalogue no. orb6492, Biorbyt, Cambridge, UK), anti-Foxo1 (1:1000; catalogue no. 82358, Thermo Fisher Scientific, Meridian Road, IL, USA), anti-phospho-Foxo1 and anti-phospho-Foxo4 (1:1000; catalogue no. #9461, Cell Signaling Technology), anti-Foxo3 (1:1000; catalogue no. NBP2-24579, Novus Biologicals, Littleton, CO, USA), anti-phospho-Foxo3 (1:1000; catalogue no. bs-3140R, Bioss, China), anti-Foxo4 (1:1000; catalogue no. bs-2766R, Bioss), anti-Fbx32/Atrogin-1 (1:1000; catalogue no. ab74023, Abcam), and anti-GAPDH (1:10 000; catalogue no. MB001H, Bioworld, St Louis Park, MN, USA). The goat anti-mouse IgG (H & L)-HRP (1:10 000; catalogue no. BS12478, Bioworld Technology, Inc.), and goat anti-rabbit IgG (H & L)-HRP (1:10 000; catalogue no. BS13278, Bioworld Technology, Inc.) were used as a secondary antibody.

Flow cytometric analysis

For the flow cytometry analysis of the cell cycle, myoblast cells were seeded in 12-well plates. When the cells grew to a density of 50% confluence, they were transfected with overexpression plasmid, siRNA, or miRNA mimics. After transfection for 48 h, the cells were collected and fixed overnight in 70% ethanol at 4°C. Subsequently, the fixed cells were stained with 50 μg/mL propidium iodide solution (Sigma Life Science, St. Louis, MO, USA) containing 10 μg/mL RNase A (Takara, Japan) and 0.2% (*v*/v) Triton X-100 (Sigma Life Science, St. Louis, MO, USA) and then incubated at 37°C in the dark for 30 min. Flow cytometry analysis was performed on a BD Accuri C6 flow cytometer (BD Biosciences, USA), and data were processed using FlowJo7.6 software.

5-Ethynyl-2′-deoxyuridine (EdU) assay

Myoblast cells were seeded in 12-well plates. When the cells grew to a density of 50% confluence, they were transfected with overexpression plasmid, siRNA, or miRNA mimics. After transfection for 48 h, myoblasts were exposed to 50 μM EdU (RiboBio, China) for 2 h at 37°C. Subsequently, the cells were fixed in 4% paraformaldehyde for 30 min, neutralized using 2 mg/mL glycine solution, and then permeabilized by adding 0.5% Triton X-100. A solution containing EdU (Apollo Reaction Cocktail; RiboBio, China) was added and the cells were incubated at room temperature for 30 min. The nuclear stain Hoechst 33342 was then added, and incubation was continued for another 30 min. A fluorescence microscope (DMi8; Leica, German) was used to capture three randomly selected fields to visualize the number of EdU-stained cells.

Cell counting kit-8 (CCK-8) assay

Primary myoblasts were seeded in 96-well plates and cultured in growth medium. After being transfected, cell proliferation was monitored using a TransDetect CCK (TransGen Biotech, Beijing, China) according to the manufacturer's protocol. Absorbance was measured using a Model 680 Microplate Reader (Bio-Rad, Hercules, California, USA) by optical density at a wavelength of 450 nm.

Lentiviral vector construction, production, and infection

LncIRS1 knockdown

Lentiviral vectors were constructed to produce lentiviruses expressing short hairpin RNA (shRNA) against *lncIRS1*. Three shRNA sequences were designed by Shanghai Hanbio Biotechnology Co., Ltd (shRNA-1: 5′-GGTCTCATGTACAACGTAT-3′, shRNA-2: 5′-GCAACTTAAAGGAAGGCAT-3′, shRNA-3: 5′-GCACAACCCTAACAGAAAT-3′). These shRNA sequences were subcloned into the pLKO.1 vector between AgeI/EcoRI restriction enzyme sites, and high titre lentiviruses were produced. Briefly, the expression vectors were co-transfected with packaging plasmid psPAX2 (Addgene, USA) and envelope plasmid pMD2.G (Addgene, USA) into 293T cells. Infectious particles were harvested at 48 and 72 h after transfection, filtered through 0.45-m-pore cellulose acetate filters, concentrated by ultracentrifugation, redissolved in sterile HBSS, aliquoted, and stored at −80°C.

LncIRS1 overexpression

For the construction of *lncIRS1*-overexpression lentiviral vector, the full-length of *lncIRS1* produced from breast muscle cDNA using PCR was subcloned into the BamHI/EcoRI restriction enzyme sites of the lentiviral expression vector (pWPXL). Lentivirus was produced as described earlier.

Lentiviral intramuscular injections

Injections were performed as previously described by Luo[20] with some modifications. Briefly, 1-day-old chicks were received three intramuscular doses (single dose injection started at Days 1, 3, and 5) of lentivirus into the breast muscle at dosage of 1×10^8 IU/mL.

Sampling and *in vivo* validation of lentiviral vectors

Breast muscle samples were taken from pLKO.1-lncIRS1 (n = 15), pLKO.1-control (n = 15), pWPXL-lncIRS1 (n = 15), and pWPXL control (n = 15) group injected chickens 9 days after the initial injection. After removing the breast muscle, 4-mm slices were taken based on designated anatomical markers using standard razor blades. Protein and RNA extraction were performed for Western blot and qPCR analysis.

Histology image analysis

Breast muscle tissues of chicken were obtained from shRNA: pLKO.1-lncIRS1, pLKO-control; and overexpression: pWPXL-lncIRS1, pWPXL-control infected muscle (n = 15/case). On Day 9 after initial dose, the tissues were quickly harvested from all groups and fixed in 10% formalin (10% formalin: 90% PBS). Fixed tissues were paraffin embedded, sectioned and stained with haematoxylin and eosin, and then subjected to image analysis.

Immunofluorescence analysis

The immunofluorescence was performed in myoblast cells cultured in 24-well plates. After transfection for 48 h, cells were fixed in 4% formaldehyde for 20 min and then washed three times with PBS (5 min each). Subsequently, the cells were permeabilized with 0.1% Triton X-100 for 15 min and

blocked with goat serum for 1 h. After overnight incubation at 4°C with anti-MyHC antibody (1:50; B103, Developmental Studies Hybridoma Bank, Iowa City, Iowa, USA), the cells were treated with Dylight 594-conjugated AffiniPure Goat Anti-Mouse IgG (H + L) (1:100; BS10027, Bioworld, USA) and incubated in dark for 1 h. The cell nuclei were visualized using DAPI staining (Beyotime, Jiangsu, China). Images were obtained with a fluorescence microscope (DMi8; Leica, German). The area of cells labelled with anti-MyHC was measured by using ImageJ software (National Institutes of Health), and the total myotube area was calculated as a percentage of the total image area covered by myotubes.

Statistical analysis

Each experiment was performed in triplicate. The data are presented as the mean ± standard error of the mean of each set of three independent experiments. Where applicable, the statistical significance of the data was tested using one-sample or paired *t*-tests. The types of tests and the *P*-values, when applicable, are indicated in the figure legends.

Results

LncRNA-miRNA-gene interaction network

There are 239 differentially expressed lncRNAs (DE-lncRNAs) (Figure 1A, Table S1) and 763 differentially expressed genes (Figure 1B, Table S2) were identified with a Benjamini *q*-value <0.001 and $|(\text{fold change})| \geq 2$ as the cut-off. Our previous study has presented the miRNA expression profile between hypertrophic and leaner broilers,[21] and 101 differentially expressed miRNAs were identified with a Benjamini *q*-value of 0.001 as the cut-off (Figure 1C, Table S3). Protein-coding RNAs (genes) and lncRNAs, which share the common MREs, can both compete for binding to miRNAs and regulate each other. In this study, we constructed a putative lncRNA-miRNA-gene crosstalk network involved in skeletal muscle myogenesis. The lncRNA-miRNA-gene crosstalk network construction involved the following three components: interactions between miRNAs and genes, interactions between lncRNAs and miRNAs, and interaction between genes and genes. Firstly, miRNA-gene interaction network contains 378 negatively correlated pairs of miRNA-gene, involving 79 miRNAs and 92 genes (Figure S2, Table S4). Secondly, the target lncRNAs of the 79 differentially expressed miRNAs from the miRNA-gene network were predicted by RNAhybrid. The lncRNA-miRNA interaction network contains 483 negatively correlated pairs of lncRNA-miRNA, involving 173 lncRNAs and 68 miRNAs (Figure S3, Table S5). Thirdly, to narrow the field of the key genes involved in skeletal muscle myogenesis, the genes of miRNA-gene network were used to construct gene–gene interactions by IPA online software. In IPA analysis, a total of four gene networks were identified (Figure S4). Importantly, one of the four gene–gene networks was involved in cellular compromise, organismal injury and abnormalities, and skeletal and muscular disorders (Figure S4c; Table S6), and 16 differentially expressed genes from this network were used for lncRNA-miRNA-gene network construction. Finally, miRNA-gene interactions, lncRNA-miRNA interactions, and gene–gene interactions were integrated to construct possible lncRNA-miRNA-gene network by Cytoscape. The lncRNA-miRNA-gene interaction network contains 733 pairs of lncRNA-miRNA-gene, involving 130 lncRNAs, 31 miRNAs, and 15 genes (Figure 1D). MiR-15 family, including miR-15a, miR-15b-5p, miR-15c-5p, miR-16-5p, and miR-16c-5p are the core component of this interaction network with a large number of genes and lncRNAs connected (Figure 1D). GO and KEGG pathway analyses of the identified genes from the lncRNA-miRNA-gene network revealed that these genes were enriched in transcription regulation-related processes, such as transcription factor activity and regulation of transcription, DNA dependent (Figure S5a). Notably, according to the KEGG analysis, *IRS1* gene from lncRNA-miRNA-gene network was enriched in skeletal muscle myogenesis related pathway, such as growth hormone signalling pathway, insulin signalling pathway, and IGF-1 signalling pathway (Figures S5b and S5c). IGF-1 signalling pathway plays a major role in the regulation of skeletal muscle myogenesis (Figure S5d). *IRS1* gene is thought to be down-stream of the *IGF1* receptor (Figure S5d), and *IRS1* null mice have much reduced growth (30–60% of control).[22,23] Interestingly, *IRS1* is the predicted target gene of miR-15 family which is the core component miRNAs in the lncRNA-miRNA-mRNA network.

LncIRS1 is up-regulated in hypertrophic broilers

RNA-seq revealed that 52 lncRNAs were down-regulated and 187 were up-regulated (Table S1) in hypertrophic and leaner broilers. We identified an lncRNA (TCONS_00086268, named *lncIRS1*) which is upregulated in hypertrophic broiler (Figure 2A and 2B). The 5′ and 3′ ends of *lncIRS1* were determined by RACE system (Figure 2C and 2D, Table S7). Predictions of the coding identify of *lncIRS1* by the Coding Potential Calculator suggested a low coding potential and low evolutionary conservation consistent with a non-coding RNA (Figure 2E).[24] In order to verify this prediction, we analysed the coding ability of seven potential ORFs of *lncIRS1*. Western blot analysis suggestive that *lncIRS1* is an lncRNA with no protein-encoding potential (Figure 2F). The NCBI BLAST indicated that the *lncIRS1* was 4623 bp long, located on Chromosome 5 and spanned from 8 080 605 to 8 085 228. We further investigated the subcellular localization of *lncIRS1*, and the RT-PCR result confirmed that it is an RNA molecule present

Figure 1 MiR-15 family is the core of lncRNA-miRNA-gene interaction network. (A) Heat map of 239 differentially expressed lncRNAs (DE-lncRNAs) between hypertrophic and leaner broilers, with rows representing lncRNAs and columns representing breast muscle tissues from WRR and XH (B) Heat map of 763 differentially expressed genes (DEGs) between hypertrophic and leaner broilers, with rows representing mRNAs and columns representing breast muscle tissues from WRR and XH. (C) Heat map of 101 differentially expressed miRNAs (DE-miRNAs) between hypertrophic and leaner broilers, with rows representing miRNAs and columns representing breast muscle tissues from WRR and XH. (D) LncRNA-miRNA-gene interaction network consists of 130 lncRNAs (green circles), 31 miRNAs (pink circles), and 15 genes (blue circles). MiR-15 family, including miR-15a, miR-15b-5p, miR-15c-5p, miR-16-5p, and miR-16c-5p are the core component of this interaction network with a large number of genes and lncRNAs connected. Dashed lines represent the interactions between differentially expressed miRNAs and theirs corresponding target genes. Solid lines represent the interactions between differentially expressed miRNAs and theirs corresponding target lncRNAs. lncRNA, long noncoding RNA; miRNA, microRNA; mRNA, messenger RNA.

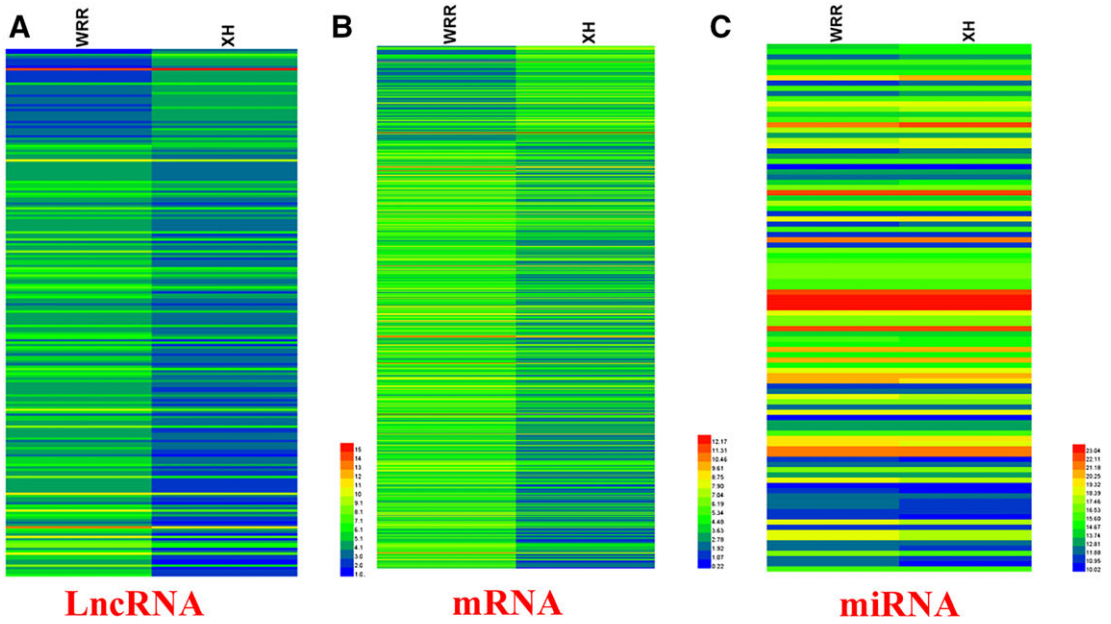

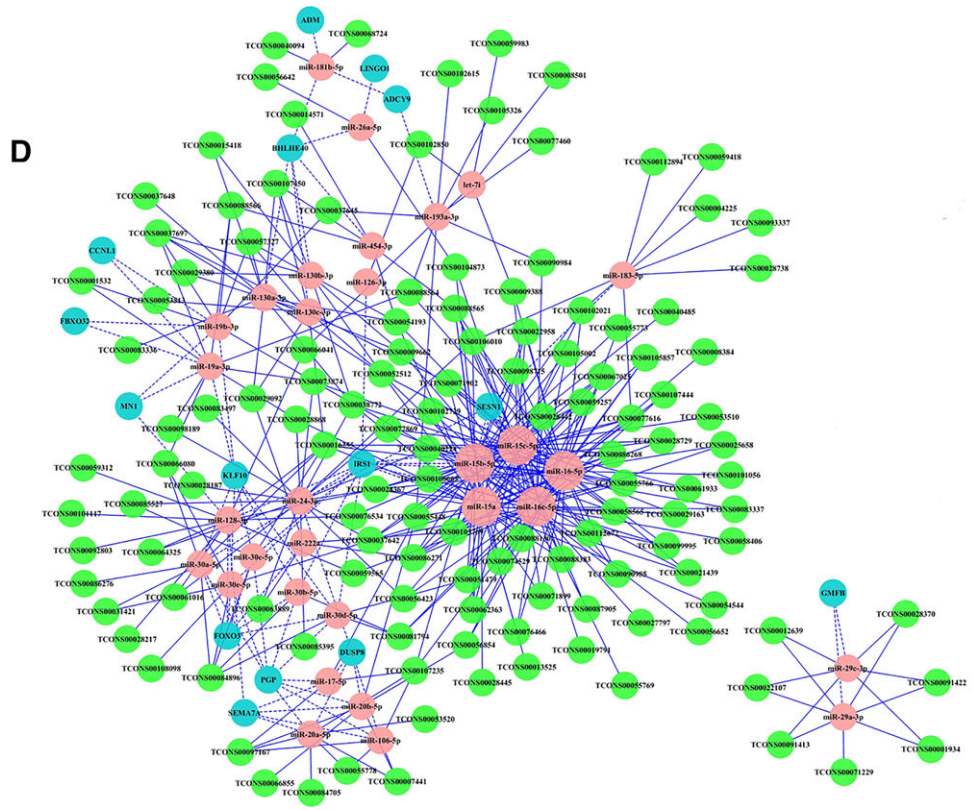

DOI: 10.1002/jcsm.12374

Figure 2 Identification of *lncIRS1*. (A) RNA sequencing found that *lncIRS1* expression was up-regulated in hypertrophic broilers compared with leaner broilers (q value=0.000652) and this expression pattern was confirmed by qPCR. The data are shown as the mean ± SEM with $*P < 0.05$ (B). (C) Results of *lncIRS1* 5′RACE. 5′RACE product, 1169 bp. (D) Result of *lncIRS1* 3′RACE. 3′RACE product, 1909 bp. (E) The coding ability predication of *lncIRS1*. Analysis was obtained from the coding potential calculator (http://cpc.cbi.pku.edu.cn/) based on evolutionary conservation and ORF attributes. (F) Western blot analysis of the coding ability of *lncIRS1*. The possible seven ORFs of *lncIRS1* were cloned into the eukaryotic expression verctor pSDS-20218 with a 3*Flag tag. Untransfected DF-1 cells were used as negative control (NC) and DF-1 cells transfected with pSDS-20218-β-actin were used as a positive control (PC). The upper panel shows the model target fragment in the pSDS vector. The lower left panel is the Western blot result of the NC and PC, and the lower right panel is the Western blot result of ORFs 1–7; all samples were probed with Flag antibody (G) *LncIRS1* is localized in the cytoplasm and nucleus. RNA was isolated from nucleus and cytoplasm fraction of myoblasts was used to analyse the expression level of *lncIRS1* by RT-PCR. GAPDH and U6 serve as cytoplasmic and nuclear localization controls, respectively. (H) Results of *IRS1* 5′RACE. 5′RACE product, 1184 bp. (I) Result of *IRS1* 3′RACE. 3′RACE product, 1075 bp. LncRNA, long noncoding RNA; RACE, rapid amplification of cDNA ends; RT-PCR, real-time PCR.

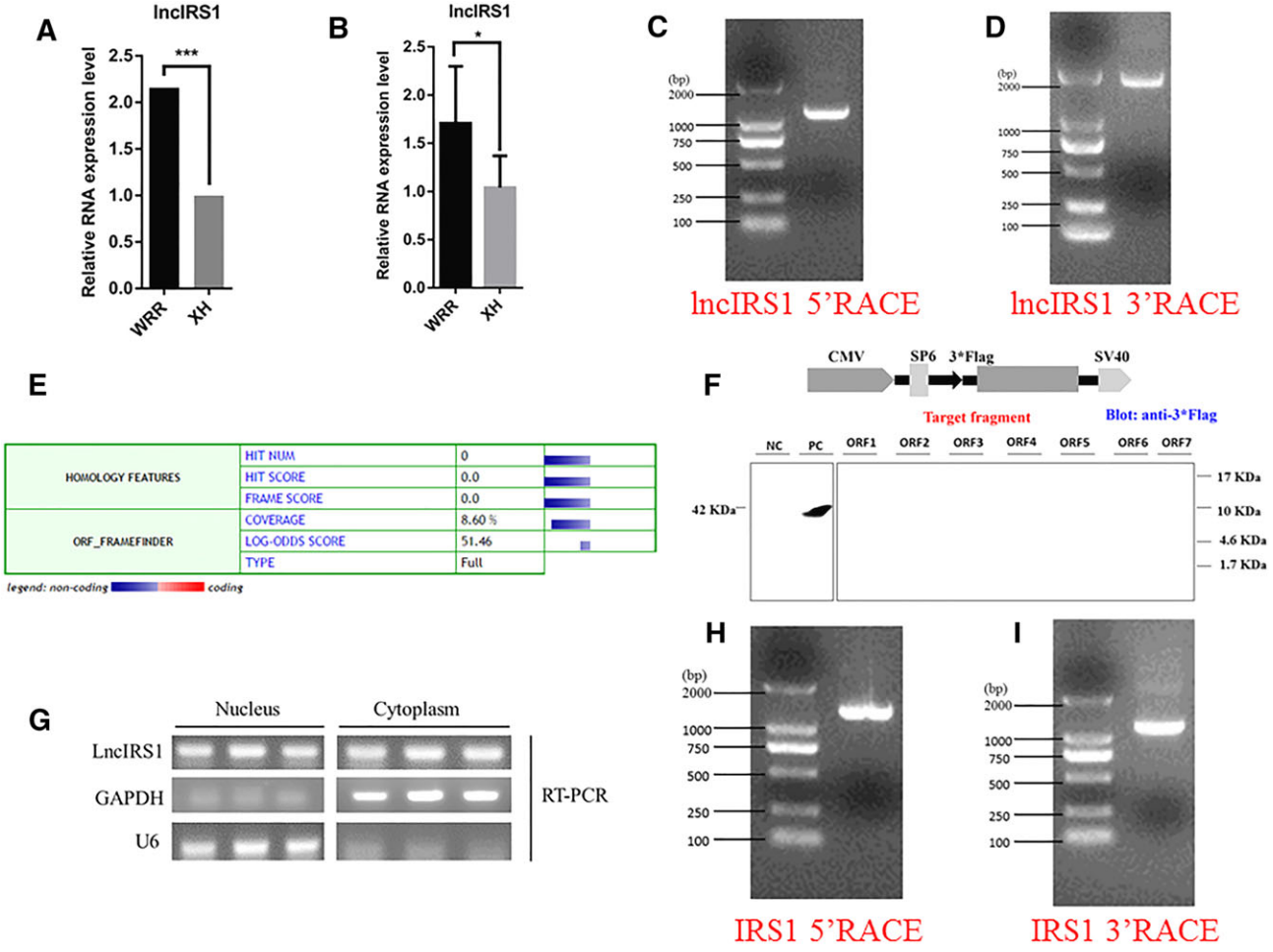

in the cytoplasm and nucleus (Figure 2G). Moreover, we identified the 5′ and 3′ ends of *IRS1* by RACE (Figure 2H and 2I, Table S7).

LncIRS1 promotes proliferation and differentiation of myoblast

LncIRS1 was predominantly expressed in breast muscle and heart and followed by liver and leg muscle (Figure 3A). During skeletal muscle development, muscle precursor cells differentiate from the somite.[25] Whole-mount *in situ* hybridization shows that *lncIRS1* is expressed in somite (Figure 3B). This may imply that *lncIRS1* plays an important role in myogenesis. Overexpression of *lncIRS1* reduced the number of cells that progressed to G0/G1 phase and increased the number of cells that progressed to S phase (Figure 3C) and significantly promoted myoblast proliferation (Figure 3D). Conversely, *lncIRS1* knockdown increased cell cycle arrest in the G0/G1 phase (Figure 3C) and significantly reduced myoblast proliferation (Figure 3E). EdU staining also demonstrated that the proliferation rate of *lncIRS1* overexpression cells was significantly increased compared with that of the control cells (Figure 3F and 3G). Conversely, proliferation was significantly inhibited

DOI: 10.1002/jcsm.12374

Figure 3 Skeletal muscle-enriched *lncIRS1* promotes myoblast proliferation and differentiation. (A) The RNA expression level of *lncIRS1* in 12 different tissues in leaner broilers. Cer, cerebrum; Ceb, cerebellum; Hyp, hypothalamus; Pit, pituitary; Abd, abdominal fat; Brm, breast muscle; Lem, leg muscle; Hea, heart; Liv, liver; Kid, kidney; Spl, spleen; Giz, gizzard. The relative RNA expression of *lncIRS1* in different tissues was normalized to Giz. (B) Whole-mount *in situ* hybridization shows that *lncIRS1* is expressed in the forming somites in HH10 chick embryo. Red arrow indicates *lncIRS1* expression location (C) Cell cycle analysis of myoblasts at 48 h after transfection of pcDNA3.1-lncIRS1 and pcDNA3.1 empty plasmid, or si-lncIRS1 and si-NC. (D) CCK-8 assay was performed to assess the effect of *lncIRS1* overexpression on myoblast proliferation. (E) CCK-8 assay was performed to assess the effect of *lncIRS1* knockdown on myoblast proliferation. (F) EdU and Hoechst (nuclei) staining analysis after transfection of pcDNA3.1-lncIRS1 and pcDNA3.1 empty plasmid, or si-lncIRS1 and si-NC in proliferating myoblast, scale bars are 50 μm. (G) The proliferation rate of myoblast cells transfected with pcDNA3.1-lncIRS1 and pcDNA3.1 empty plasmid, or si-lncIRS1 and si-NC. (H, I) Immunofluorescence Myoblast cells transfected with pcDNA3.1-lncIRS1 and pcDNA3.1 empty plasmid, or si-lncIRS1 and si-NC were induced to differentiate for 72 hr then stained with MyHC antibody and DAPI (nuclei). Scale bars are 100 μm. (J, K) Myotube area (%) at 72 h after transfection of pcDNA3.1-lncIRS1 or si-lncIRS1. (L) Knockdown of *lncIRS1* decreased the RNA expression level of myoblast cell differentiation associated genes, including *MyoD*, *MyoG*, *MyHC*, and *MyoMarker*. (M) Knockdown of *lncIRS1* decreased the RNA expression level of IGF-1 pathway associated genes, including *IGF1*, *IGF1R*, and *IGF2R*. Results are shown as the mean ± SEM of three independent experiments. Independent sample *t*-test was used to analysis the statistical differences between groups. * $P < 0.05$, ** $P < 0.01$, *** $P < 0.001$, and **** $P < 0.0001$.

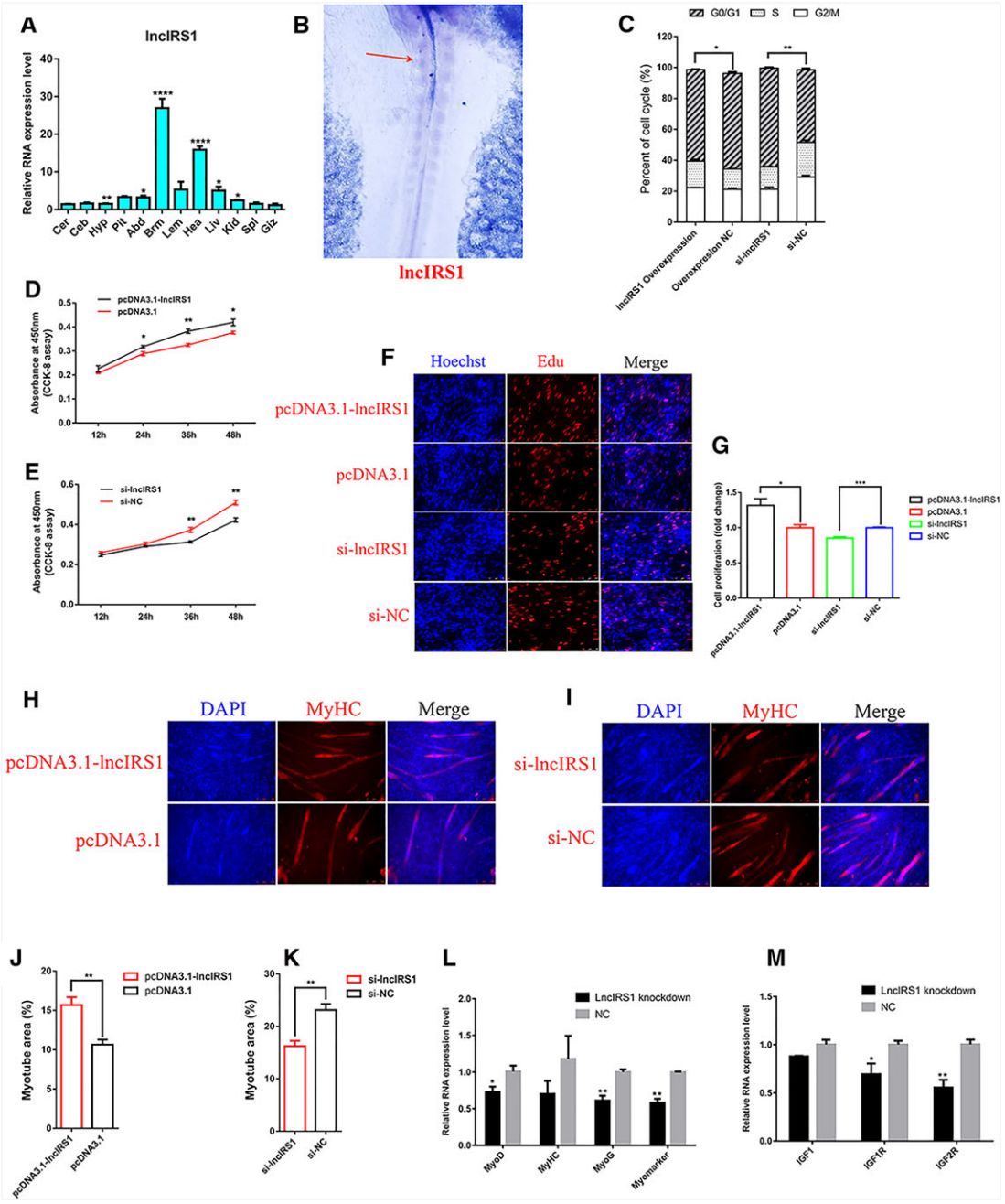

DOI: 10.1002/jcsm.12374

after *lncIRS1* knockdown (Figure 3F and 3G). After immunofluorescence staining, we found *lncIRS1* overexpression promoted myoblast differentiation and significantly increased the total areas of myotubes (Figure 3H and 3J), while knockdown of *lncIRS1* reduced myoblast differentiation (Figure 3I and 3K). The expression of myoblast differentiation marker genes (*MyoD*, *MyHC*, *MyoG*, and *Myomarker*) and IGF-1 pathway related genes (*IGF1*, *IGF1R*, and *IGF2R*) were down-regulated in *lncIRS1* knockdown cells compared to control cells (Figure 3L and 3M). Together, the data suggest that *lncIRS1* enriched in muscle and can promote myoblast proliferation and differentiation.

LncIRS1 acts as a molecular sponge for miR-15a, miR-15b-5p, and miR-15c-p to regulate IRS1 expression

LncIRS1 locates in both cytoplasm and nucleus (Figure 2G), and it is significantly upregulated in hypertrophic broiler. We speculated that *lncIRS1* regulate myogenesis by function as a ceRNA. In lncRNA-miRNA-gene network, miR-15 family is the core component of this network, and *IRS1* is a target gene of these miRNAs. Interestingly, bioinformatics analysis reveals three or one predicted miRNA binding site in the *lncIRS1* (Figure 4A) or *IRS1* (Figure 4B), respectively. During myoblast proliferation and differentiation, *IRS1* (Figure 4C) and *lncIRS1* (Figure 4D) RNA expression level were upregulated, while the opposite expression pattern was presented in miR-15a (Figure 4E), miR-15b-5p (Figure 4F), and miR-15c-5p (Figure 4G) but not miR-16-5p (Figure 4H) or miR-16c-5p (Figure 4I). Using dual-luciferase reporter gene assays, we validated that miR-15a, miR-15b-5p, and miR-15c-5p can directly interact with the three predicted binding sites of *lncIRS1* (Figure 4J–4L), and these miRNAs can also directly interact with *IRS1* (Figure 4M). To determine whether *lncIRS1* could regulate *IRS1* expression by sequester miRNAs, we co-transfected pmirGLO-IRS1, miRNAs, and *lncIRS1* overexpression plasmid into DF-1 cells. The luciferase activity increased in response to *lncIRS1* in a dose-dependent manner, suggesting that ectopically expressed *lncIRS1* specifically sequestered miR-15a (Figure 4N), miR-15b-5p (Figure 4O), and miR-15c-5p (Figure 4P), thereby preventing theirs from inhibiting luciferase activity. Overexpression of these miRNAs could simultaneously reduce the expression of *lncIRS1* (Figure 4Q, Figure S6a) and *IRS1* (Figure 4R, Figure S6b). We further performed RNA immunoprecipitation using antibody against AGO2 which is a key component of the RNA-induced silencing complex. As expected, *lncIRS1* (Figure 4S), *IRS1* (Figure 4T), miR-15a, miR-15b-5p, and miR-15c-5p (Figure 4U) were significantly enriched in AGO2 pellet (AGO2 antibody versus IgG). Western blot confirmed that the AGO2 antibody precipitated the AGO2 protein from our cellular extract (Figure 4V). Overexpression of miR-15a, miR-15b-5p, and miR-15c-5p can significantly reduce the protein level of *IRS1* (Figure 4W). Together, these data suggest that *lncIRS1* can regulate the expression of *IRS1* by sequester miR-15a, miR-15b-5p, and miR-15c-5p.

MiR-15a, miR-15b-5p, and miR-15c-5p suppress myoblast proliferation and differentiation

We identified miR-15a, miR-15b-5p, and miR-15c-5p are down-regulated in hypertrophic broiler (Figure 5A and 5B). To observe the effects of these miRNAs on myoblast proliferation, we transfected myoblasts with miRNA mimics or miRNA negative control (miR-NC) and then monitored the proliferation status of cells using flow cytometry analysis, CCK-8 assay, and EdU staining. Flow cytometry analysis of the cell cycle revealed that myoblasts transfected with the miR-15a, miR-15b-5p, or miR-15c-5p mimic could arrest myoblasts in the G0/G1 phase (Figure 5C). CCK-8 and EdU staining also demonstrated that the proliferation rate of miR-15a, miR-15b-5p, or miR-15c-5p transfected myoblasts was significantly reduced compared with that of the miR-NC transfected cells (Figure 5D–5F). After immunofluorescence staining, we found miR-15a, miR-15b-5p, or miR-15c-5p overexpression inhibited myoblast differentiation and significantly reduced the total areas of myotubes (Figure 5G and 5H). The expression of IGF-1 pathway related genes (*IGF1*, *IGF1R*, and *IGF2R*) and myoblast differentiation marker genes (*MyoD*, *MyHC*, *MyoG*, and *Myomarker*) were down-regulated in miR-15a, miR-15b-5p, or miR-15c-5p overexpression myoblasts compared to miR-NC transfected myoblasts (Figure 5I–5O). Overexpression of miR-15a, miR-15b-5p, or miR-15c-5p reduced the protein expression level of MyoG and MyHC. The kinase AKT is a central component in IGF-1 signalling pathway which plays a major role in the regulation of skeleteal muscle growth. As shown in Figure 4W, overexpression of miR-15a, miR-15b-5p, or miR-15c-5p reduced the phosphorylation level of AKT and had no obvious change in total AKT. Together, the data suggest that miR-15a, miR-15b-5p, and miR-15c-5p inhibit myoblast proliferation and differentiation via IGF-1 pathway.

IRS1 is involved in proliferation and differentiation of myoblast via IGF-1 signalling pathway

IRS1 is thought to be downstream of the IGF-1 receptor and associated with mice body weight.[7] Here, we identified *IRS1* is upregulated in hypertrophic broiler (Figure 6A and 6B), and predominantly expressed in skeletal muscle (Figure 6C). Whole-mount *in situ* hybridization shows that *IRS1* is expressed in somite (Figure 6D), which is consistent with *lncIRS1* (Figure 3B). Overexpression of *IRS1* reduced the number of cells that progressed to G0/G1 phase, increased the

Figure 4 *LncIRS1* functions as a ceRNA for miR-15a, miR-15b-5p, and miR-15c-5p. (A) Three miR-15 family binding sites in *lncIRS1* were identified by RNAhybrid. (B) The miR-15 family binding site in *IRS1* was identified by TargetScan. Expression analysis of *IRS1* (C), *lncIRS1* (D), miR-15 a (E), miR-15b-5p (F), miR-15c-5p (G), miR-16-5p (H), and miR-16c-5p (I) during myoblasts proliferation (GM) and differentiation (DM), using qRT-PCR. The dual-luciferase reporter assay verified that Site 1 (position 2651–2657 of *lncIRS1*) (J), Site 2 (position 3438–3444 of *lncIRS1*) (K) and Site 3 (position 3775–3781 of *lncIRS1*) (L) of *lncIRS1* could be bound by miR-15a, miR-15b-5p, and miR-15c-5p. (M) The dual-luciferase reporter assay verified that *IRS1* could be bound by miR-15a, miR-15b-5p, and miR-15c-5p; pmirGLO-IRS1 or miR-15a (N), miR-15b-5p (O), and miR-15c-5p (P) were transfected into DF-1 cells, together with 0, 25, 50, or 100 ng of sponge plasmid of *lncIRS1*. Overexpression of miR-15a, miR-15b-5p, or miR-15c-5p decreased the RNA expression level of *lncIRS*1 (Q) and *IRS1* (R). Association of *lncIRS1*, *IRS1*, and miR-15a, miR-15b-5p, and miR-15c-5p with AGO2. Cellular lysates from chicken myoblast cells were used for RNA immunoprecipitation with AGO2 antibody. Detection of *lncIRS1* (S); *IRS1* (T); miR-15a, miR-15b-5p, and miR-15c-5p (U) using qRT-PCR; and detection of AGO2 using IP-Western analysis (V). (W) Overexpression of miR-15a, miR-15b-5p, and miR-15c-5p decreased the protein expression level of IRS1, p-AKT, MyoG, and MyHC. Results are shown as the mean ± SEM of three independent experiments. Independent sample *t*-test was used to analysis the statistical differences between groups. * $P < 0.05$, ** $P < 0.01$, *** $P < 0.001$, and **** $P < 0.0001$. RIP, RNA immunoprecipitation.

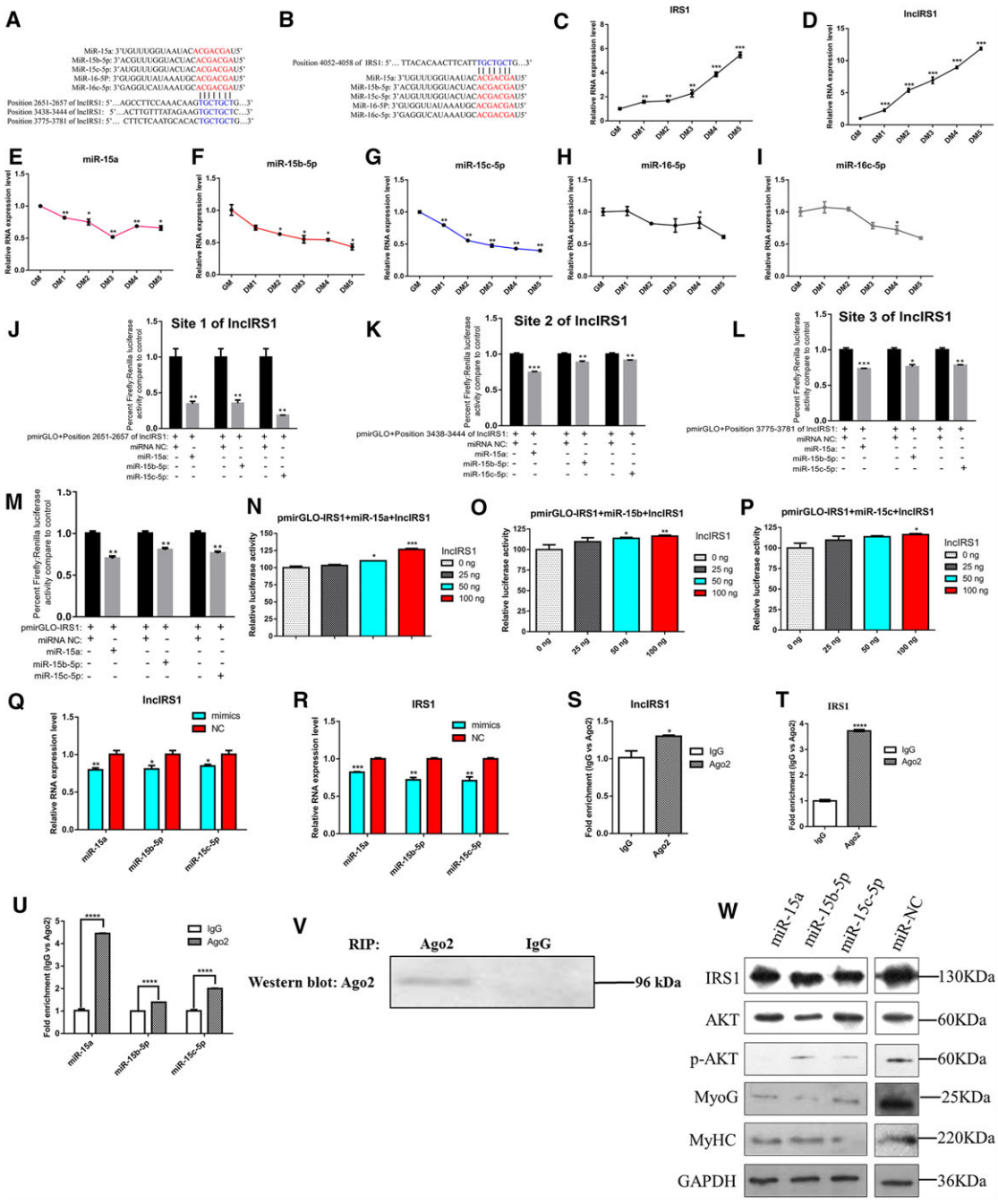

DOI: 10.1002/jcsm.12374

Figure 5 MiR-15a, miR-15b-5p, and miR-15c-5p inhibit myoblast proliferation and differentiation. (A) RNA-seq analysis found that miR-15a, miR-15b-5p, and miR-15b-5p were down-regulated in hypertrophic broilers compared with leaner broilers, and this expression pattern was validated by qRT-PCR (B). (C) Cell cycle analysis of myoblasts at 48 h after transfection of miR-15a, miR-15b-5p, miR-15c-5p, and miR-NC. (D) CCK-8 assay was performed to assess the effect of miR-15a, miR-15b-5p, or miR-15c-5p overexpression on myoblast proliferation. (E) EdU and Hoechst (nuclei) staining analysis after transfection of miR-15a, miR-15b-5p, or miR-15c-5p in proliferating myoblast, scale bars are 50 μm. (F) The proliferation rate of myoblast cells transfected with miR-15a, miR-15b-5p, or miR-15c-5p. (G) Myoblast cells transfected with miR-15a, miR-15b-5p, or miR-15c-5p were induced to differentiate for 72 hr then stained with MyHC antibody and DAPI (nuclei). Scale bars are 100 μm. (H) Myotube area (%) at 72 h after transfection of miR-15a, miR-15b-5p, or miR-15c-5p. Overexpression of miR-15a, miR-15b-5p, or miR-15c-5p decreased the RNA expression level of IGF-1 pathway associated genes, including *IGF1* (I), *IGF1R* (J), and *IGF2R* (K). Overexpression of miR-15a, miR-15b-5p, or miR-15c-5p decreased the RNA expression level of myoblast cell differentiation associated genes, including *MyoD* (L), *MyoG* (M), *MyHC* (N), and *MyoMarker* (O). Results are shown as the mean ± SEM of three independent experiments. Independent sample *t*-test was used to analysis the statistical differences between groups. * $P < 0.05$, ** $P < 0.01$, *** $P < 0.001$, and **** $P < 0.0001$.

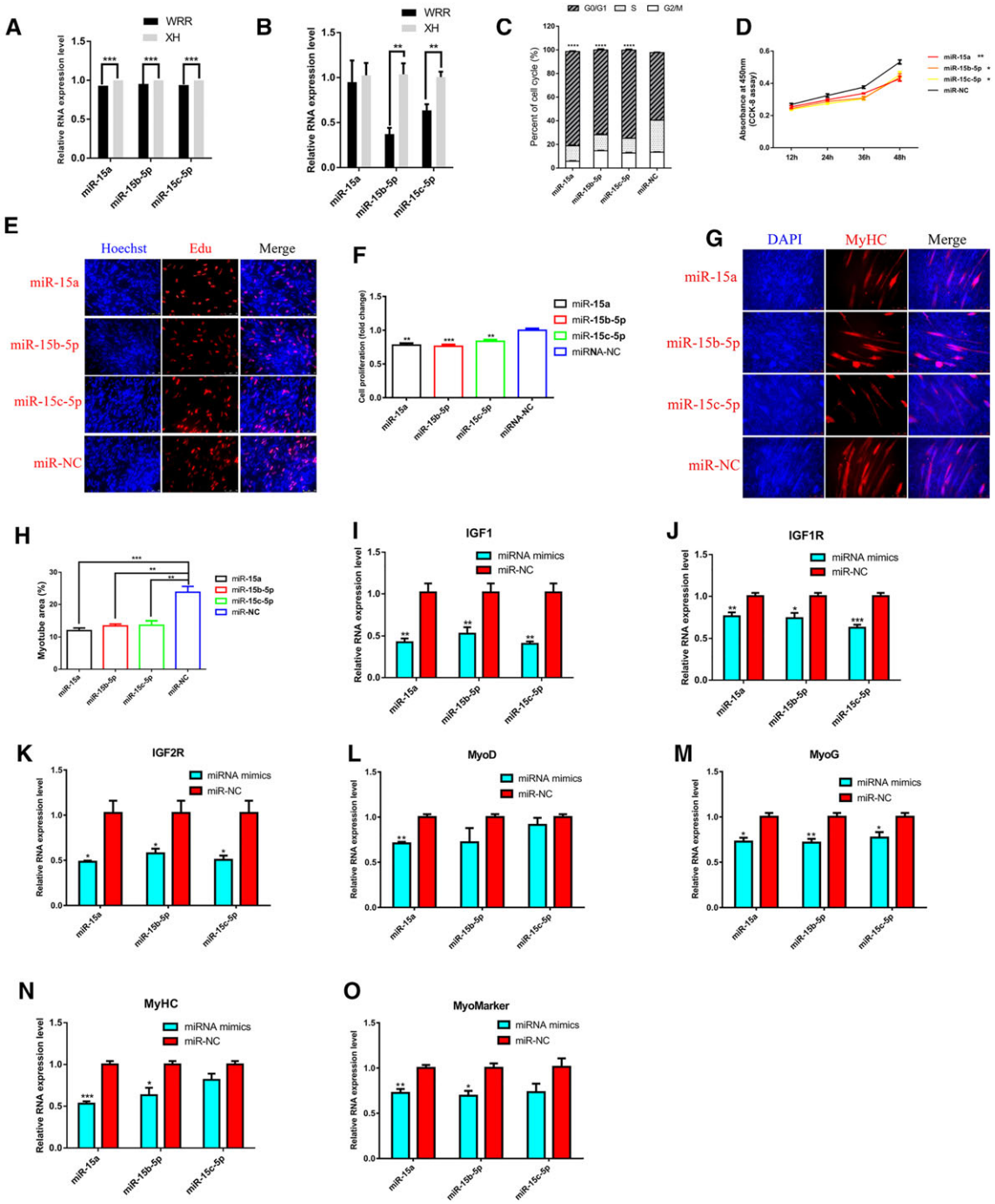

DOI: 10.1002/jcsm.12374

Figure 6 *IRS1* promotes myoblast proliferation and differentiation. (A) RNA-seq analysis found that *IRS1* was up-regulated in hypertrophic broilers, and this expression pattern was validated by qRT-PCR (B). (C) The RNA expression level of *IRS1* in 12 different tissues in leaner broilers and expression was normalized to Giz. (D) Whole-mount *in situ* hybridization showed that *IRS1* are expressed in the forming somites in HH10 chick embryo Red arrow indicates IRS1 expression location. (E) Cell cycle analysis of myoblasts at 48 h after transfection of pcDNA3.1-IRS1 and pcDNA3.1 empty plasmid, or si-IRS1 and si-NC. (F) CCK-8 assay was performed to assess the effect of *IRS1* overexpression on myoblast proliferation. (G) CCK-8 assay was performed to assess the effect of *IRS1* knockdown on myoblast proliferation. (H) EdU and Hoechst (nuclei) staining analysis after transfection of pcDNA3.1-IRS1 and pcDNA3.1 empty plasmid, or si-IRS1 and si-NC in proliferating myoblast, scale bars are 50 μm. (I) The proliferation rate of myoblast cells transfected with pcDNA3.1-IRS1 and pcDNA3.1 empty plasmid, or si-IRS1 and si-NC. (J, L) Myoblast cells transfected with pCDNA3.1-IRS1, or si-IRS1 were induced to differentiate for 72 hr then stained with MyHC antibody and DAPI (nuclei). Scale bars are 100 μm. (K, M) Myotube area (%) was determined at 72 h after transfection of pcDNA3.1-IRS1 or si-IRS1. (N) Knockdown of *IRS1* decreased the RNA expression level of myoblast cell differentiation associated genes, including *MyoD*, *MyoG*, *MyHC*, and *MyoMarker*. (O) Knockdown of *IRS1* decreased the RNA expression level of IGF-1 pathway associated genes, including *IGF1*, *IGF1R*, and *IGF2R*. Results are shown as the mean ± SEM of three independent experiments. Independent sample *t*-test was used to analysis the statistical differences between groups. * $P < 0.05$, ** $P < 0.01$, *** $P < 0.001$, and **** $P < 0.0001$.

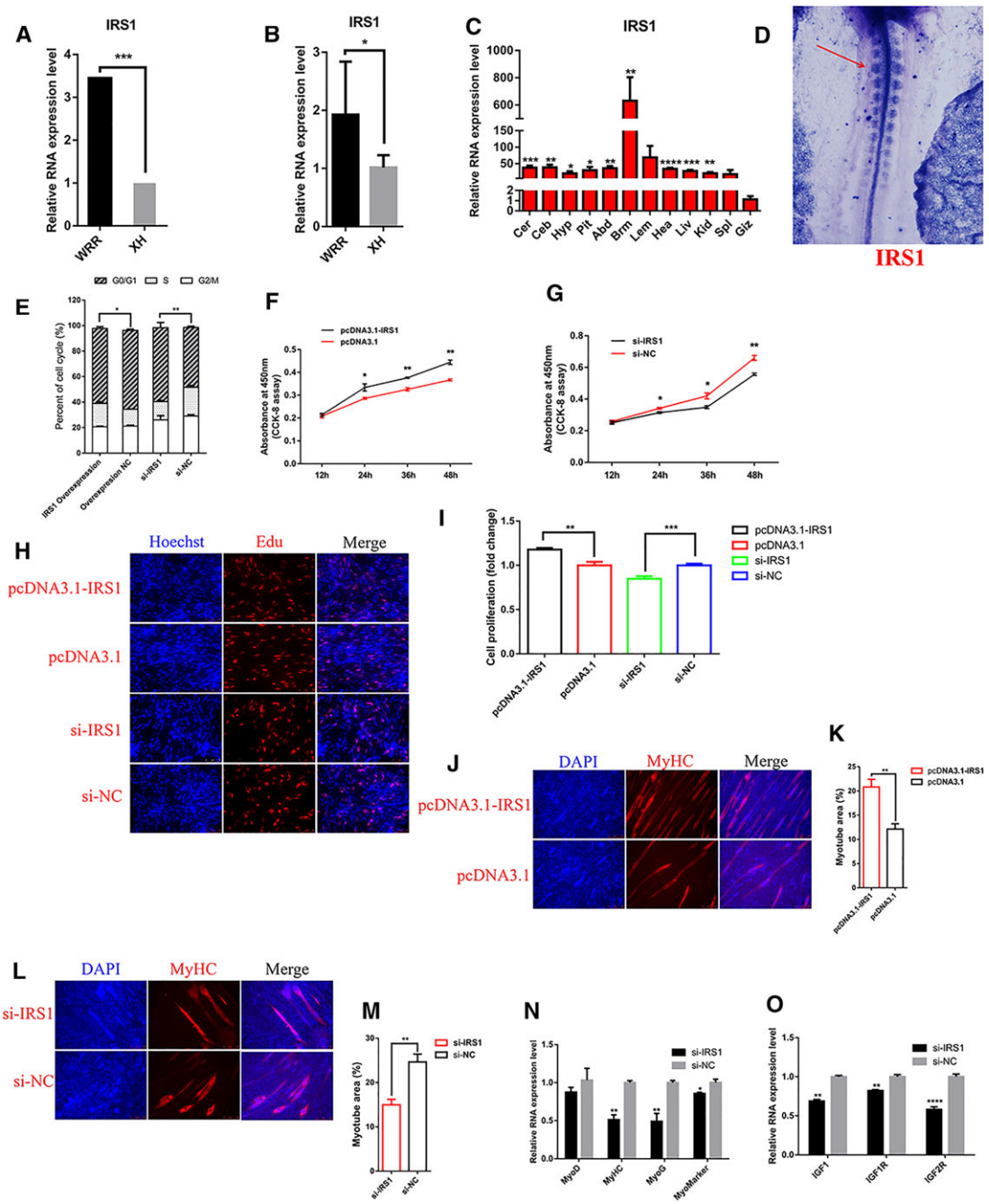

DOI: 10.1002/jcsm.12374

number of cells that progressed to S phase (Figure 6E), and significantly promoted myoblast proliferation (Figure 6F). Conversely, *IRS1* knockdown increased cell cycle arrest in the G0/G1 phase (Figure 6E) and significantly reduced myoblast proliferation (Figure 6G). EdU staining also demonstrated that the proliferation rate of *IRS1* overexpression cells was significantly increased compared with that of the control cells (Figure 6H and 6I). Conversely, proliferation was significantly inhibited after *IRS1* knockdown (Figure 6H and 6I). After immunofluorescence staining, we found *IRS1* overexpression promoted myoblast differentiation and significantly increased the total areas of myotubes (Figure 6J and 6K), while knockdown of *IRS1* reduced myoblast differentiation (Figure 6L and 6M). The expression of myoblast differentiation marker genes (*MyoD*, *MyHC*, *MyoG*, and *Myomarker*) and IGF-1 pathway related genes (*IGF1*, *IGF1R*, and *IGF2R*) were down-regulated in *IRS1* knockdown cells compared to control cells (Figure 6N and 6O). Together, these data suggest that *IRS1* promotes myoblast proliferation and differentiation via IGF-1 pathway.

LncIRS1 modulated IRS1 expression and promoted myoblast proliferation and differentiation by sponging miR-15a, miR-15b-5p, and miR-15c-p

To determine whether *lncIRS1* functions as a molecular sponge for miR-15a, miR-15b-5p, and miR-15c-p, we performed qPCR analysis of *lncIRS1* and *IRS1* level in *lncIRS1* or *IRS1* knockdown myoblast, respectively. Knockdown of *lncIRS1* reduce the expression level of *lncIRS1* and simultaneously inhibit *IRS1* expression (Figure 7A). Similarly, knockdown of *IRS1* reduce the expression level of *IRS1* and *lncIRS1* (Figure 7B). Furthermore, the rescue assay shown that *lncIRS1* overexpression can promote the expression of *IRS1* (Figure 7C, Figure S6c). Overexpression of *lncIRS1* (OV-lncIRS1) increased the protein level of *IRS1* (Figure 7D), as the same effect of *IRS1* transfected (OV-IRS1). Overexpression of *lncIRS1* increased the phosphorylation level of AKT, which confirmed that *lncIRS1* activates the IGF-1 pathway via IRS1 protein. Overexpression of *lncIRS1* promotes the myoblast differentiation marker genes (*MyoG* and *MyHC*) expression (Figure 7D). The opposite results were observed by knockdown of *lncIRS1* or *IRS1* (Figure 7E). These data demonstrated that *lncIRS1* modulates *IRS1* to activate the IGF-1 signalling pathway, affecting myoblast proliferation and differentiation by sponge miR-15a, miR-15b-5p, and miR-15c-p.

LncIRS1 could rescue skeletal muscle atrophy

We first investigated the impact of *lncIRS1* and miR-15 family on atrophy-related gene expressions in primary myotubes. *LncIRS1* overexpression decreased the expression of two atrophy-related genes (atrogenes), *Atrogin-1* and *MuRF1*, at either mRNA levels or protein level of Atrogin-1 compared to the control group (Figure 7F–7H). In contrast, myotubes transfected with *lncIRS1* knockdown increased the expression of *Atrogin-1* and *MuRF1* at either mRNA levels or protein level of Atrogin-1 compared to those transfected with the small interfering RNA negative control (Figure 7F, 7I, and 7J). In addition, overexpression of miR-15a, miR-15b-5p, or miR-15c-5p promotes the protein expression of Atrogin-1 (Figure 7F).

The dexamethasone (synthetic glucocorticoid) has been known to promote protein breakdown and to induce *Atrogin-1* and *MuRF1* expression in myotube cultures and adult muscles.[26,27] IGF downstream signalling (AKT-FOXO signalling) has been reported to play a major role in eliciting the myofiber atrophy.[28] We next asked if *lncIRS1* rescue muscle atrophy, we performed *lncIRS1* overexpression and knockdown during dexamethasone-induced myotube atrophy *in vitro*. We then assessed AKT and FOXO signalling by determining the levels of Foxo1, phosphorylated Foxo1 (p-Foxo1), Foxo3, phosphorylated Foxo3 (p-Foxo3), Foxo4, phosphorylated Foxo4 (p-Foxo4), AKT, phosphorylated AKT (p-AKT), and Atrogin-1 by Western blot analysis. Result showed that protein expression of p-Foxo1, p-Foxo3, p-Foxo4, and p-AKT in dexamethasone-treated myotubes was increased after transfection with *lncIRS1* overexpression plasmid (OV-lncIRS1) compared with control (OV-NC) (Figure 8A–8E). The protein expression level of Atrogin-1 was decreased in *lncIRS1* overexpression group (Figure 8F). In contrast, the protein expression (p-Foxo1, p-Foxo3, p-Foxo4, and p-AKT) was decreased after interference with si-lncIRS1 (Figure 8G–8K). The protein expression level of Atrogin-1 was increased in si-lncIRS1 group (Figure 8L). Taken together, our data demonstrated that *lncIRS1* regulates the expression of atrophy-related genes and further can rescue dexamethasone-induced atrophy in cultured myotubes.

LncIRS1 controls muscle mass and muscle fibre cross-sectional area

To test whether *lncIRS1* regulates muscle growth *in vivo*, 1-day-old chicks were injected with lentiviral-mediated *lncIRS1* overexpression (pWPXL-lncIRS1) and lentiviral-mediated *lncIRS1* knockdown (pLKO.1-lncIRS1). Compared with control group (pWPXL-control), the expression level of *lncIRS1* or *IRS1* gene was significantly higher in pWPXL-lncIRS1 (Figure 9A and 9B). Breast muscle mass (breast muscle weight) and muscle fibre cross-sectional area were both increased in the *lncIRS1* overexpression groups compared with those in control groups (Figure 9C–9E), while they were decreased in *lncIRS1* knockdown groups (Figure 9F–9J). In addition, we performed Western blot analysis

Figure 7 *LncIRS1* promotes myoblast differentiation via IGF-1 signalling pathway. (A) mRNA expression of *lncIRS1* and *IRS1* after *lncIRS1* knockdown in myoblasts. (B) mRNA expression of *lncIRS1* and *IRS1* after *IRS1* knockdown in myoblasts. (C) Co-expression of miR-15a, miR-15b-5p, or miR-15c-5p with *lncIRS1* up-regulated the expression level of *IRS1*. (D) Overexpression of *lncIRS1* or *IRS1* increased the protein expression level of IRS1, p-AKT, MyoG, and MyHC. (E) Knockdown of *lncIRS1* or *IRS1* reduced the protein expression level of *IRS1*, p-AKT, MyoG, and MyHC. (F) Effect of *lncIRS1* overexpression, *lncIRS1* knockdown, and miR-15 family on Atrogin-1 protein expression. (G) Effect of *lncIRS1* overexpression on *Atrogin-1* RNA expression. (H) Effect of *lncIRS1* overexpression on *MuRF*1 RNA expression. (I) Effect of *lncIRS1* knockdown on *Atrogin-1* RNA expression. (J) Effect of *lncIRS1* knockdown on *MuRF1* RNA expression in all panels, Myoblast cells transfected with above-indicated chemicals (plasmid DNA, siRNAs, or miRNAs) were induced to differentiate for 48 hr then detected with qRT-PCR or Western blot analysis. Results are shown as the mean ± SEM of three independent experiments. Independent sample *t*-test was used to analysis the statistical differences between groups. * $P < 0.05$, ** $P < 0.01$, *** $P < 0.001$, and **** $P < 0.0001$.

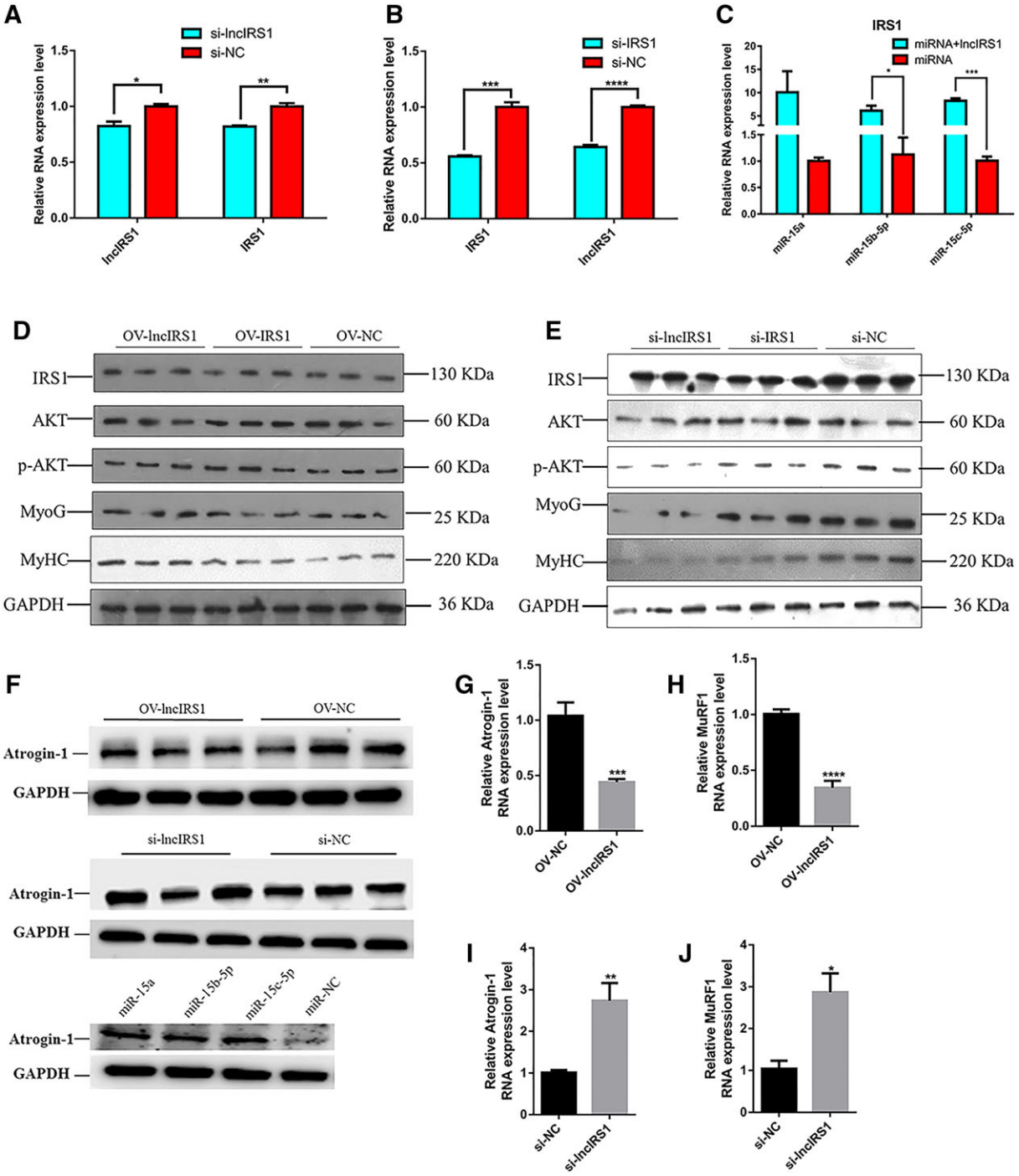

DOI: 10.1002/jcsm.12374

Figure 8 *LncIRS1* could rescue skeletal muscle atrophy. (A) Effect of *lncIRS1* overexpression on AKT-FOXO signalling pathway. Chicken primary myotubes isolated from leg muscle of E11 were first treated with dexamethasone for 24 hr to induce atrophy and then transfected with *lncIRS1* overexpression plasmid for 48 hr, followed by Western blot analysis. (B–E) Effect of *lncIRS1* overexpression on protein phosphorylation level of AKT-FOXO signalling pathway components, including p-foxo1 (B), p-foxo3 (C), p-foxo4 (D), and p-AKT (E). (F) Effect of *lncIRS1* overexpression on protein expression level of Atrogin-1 during dexamethasone treated myotubes. (G) Effect of *lncIRS1* knockdown on AKT-FOXO signalling pathway. Chicken primary myotubes isolated from leg muscle of E11 were first treated with dexamethasone for 24 hr to induce atrophy and then transfected with si-lncIRS1 for 48 hr, followed by Western blot analysis. (H–K) Effect of *lncIRS1* knockdown on protein phosphorylation level of AKT-FOXO pathway, contains p-foxo1 (H), p-foxo3 (I), p-foxo4 (J), and p-AKT (K). (L) Effect of *lncIRS1* knockdown on Atrogin-1 protein expression level during dexamethasone treated myotubes. In all panels, error bars indicate the standard error of the mean. Independent sample *t*-test was used to analysis the statistical differences between groups. * $P < 0.05$, ** $P < 0.01$, and *** $P < 0.001$.

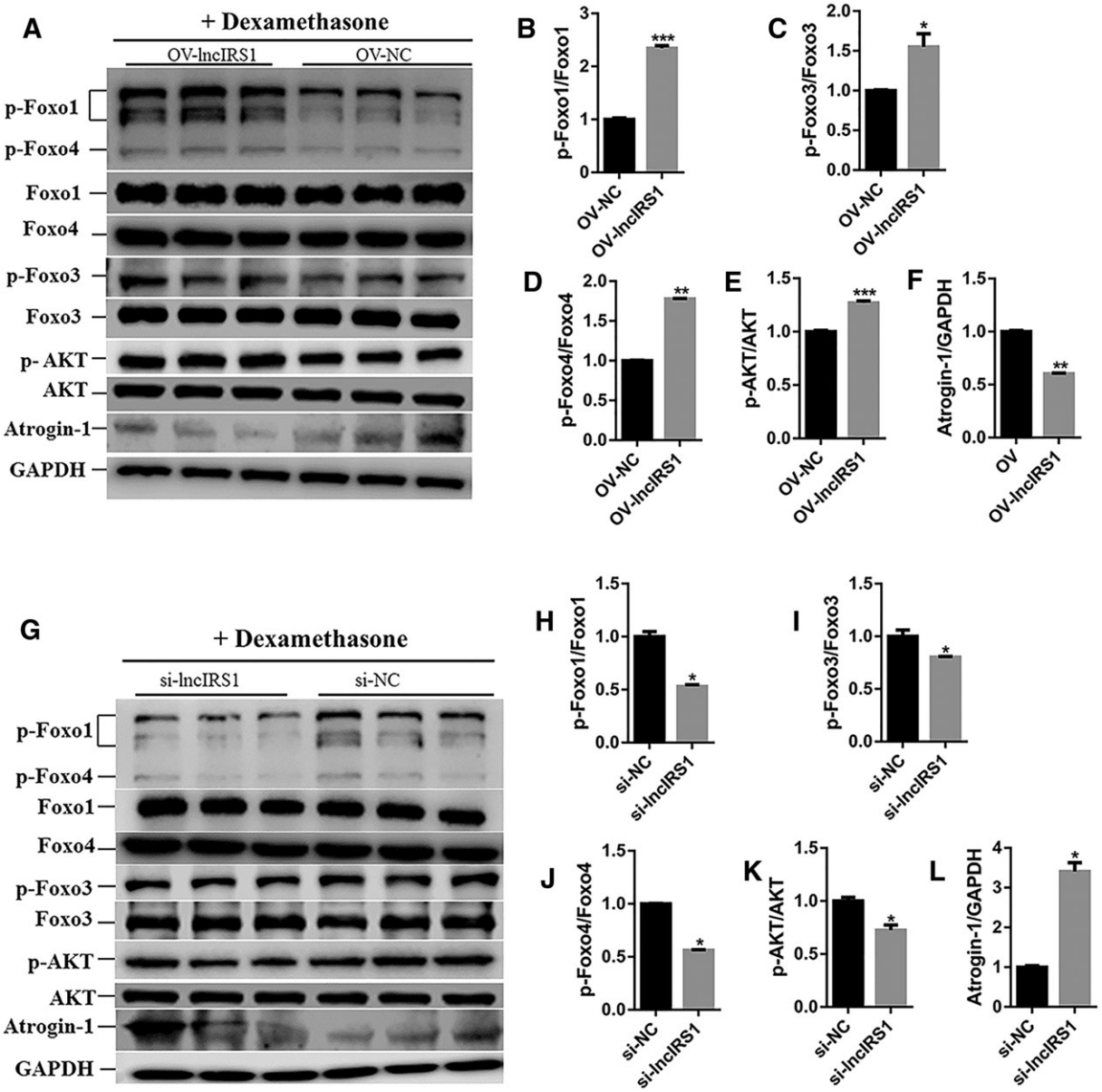

for AKT-FOXO signalling in lentiviral-*lncIRS1* overexpression and knockdown. The results showed that protein expression of p-Foxo1, p-Foxo3, p-Foxo4, and p-AKT in *lncIRS1* overexpression group (pWPXL-lncIRS1) had higher level than did control group (pWPXL-control), while *lncIRS1* knockdown group (pLKO.1-lncIRS1) had lower expression level than did the controls (pLKO.1-control) (Figure 9K). Moreover, the protein levels of myogenic markers (MyoG and MyHC) showed similar changes with the parameters of breast muscle mass (Figure 9K). We conclude that *lncIRS1* is associated with muscle mass and muscle fibre *in vivo*.

Figure 9 *LncIRS1* regulates muscle mass and mean muscle fibre *in vivo*. (A) qRT-PCR of *lncIRS1* after *lncIRS1* overexpression prepared with lentivirus and intramuscularly injected into the breast muscle. (B) qRT-PCR of *IRS1* after *lncIRS1* overexpression prepared with lentivirus and intramuscularly injected into the breast muscle. (C–E) Breast muscle weight (C), mean muscle fibre cross-section area (CSA) (D), and H-E staining (E) of breast muscle fibre cross section infected with pWPXL-lncIRS1 or pWPXL-control scale bars are 50 μm. (F) qRT-PCR analysis of *lncIRS1* expression in pLKO.1-lncIRS1 overexpression group or pLKO.1-control group prepared with lentivirus and intramuscularly injected into the chicken breast muscle. (G) qRT-PCR analysis of *IRS1* expression in pLKO.1-lncIRS1 overexpression group or pLKO.1-control group prepared with lentivirus and intramuscularly injected into the chicken breast muscle. (H–J) Breast muscle weight (H), mean muscle fibre cross-section area (CSA) (I), and H-E staining (J) of breast muscle fibre cross section infected with pLKO.1-lncIRS1 or pLKO.1-control scale bars are 50 μm. (K) The protein expression level of AKT-FOXO signalling components and myogenic-related markers (MyoG and MyHC) during chicken infection with lentivirus containing pWPXL-lncIRS1 and pWPXL-control, or pLKO.1-lncIRS1 and pLKO.1-control, as analysed by Western blot. (L) Molecular mechanism of *lncIRS1* promotes myoblast proliferation, differentiation, and muscle fibre. *LncIRS1* controls IRS1 protein level and further activates IGF-1 signalling pathway by functioning as ceRNA to sponge miR-15a, miR-15b-5p, and miR-15c-5p. In all panels, error bars indicate the standard error of the mean. Independent sample *t*-test was used to analysis the statistical differences between groups. * $P < 0.05$, ** $P < 0.01$, *** $P < 0.001$, and **** $P < 0.0001$.

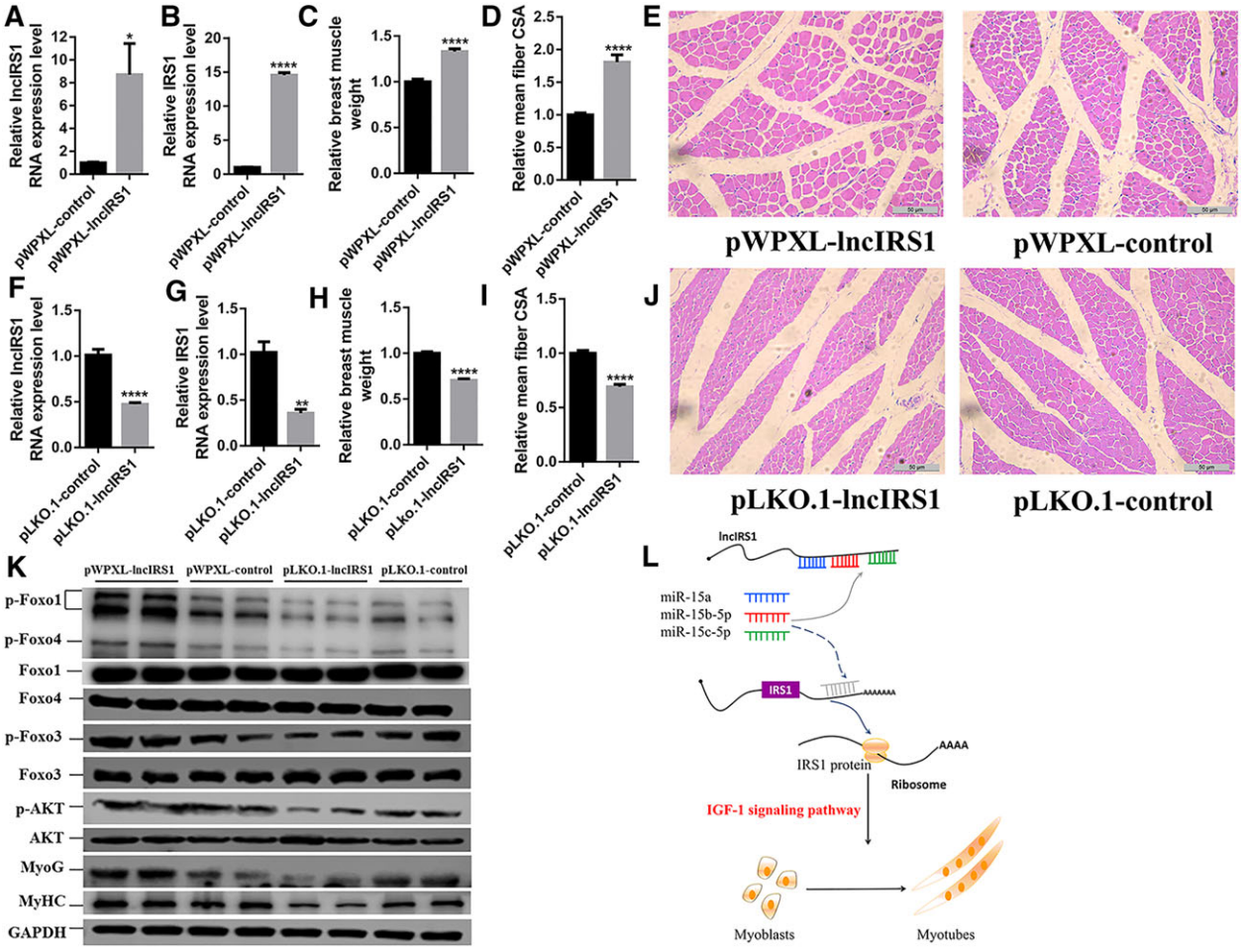

Discussion

In recent years, studies revealed that lncRNAs containing MREs act as molecular sponges to effectively inhibit miRNA function.[29,30] *Lnc-mg* promotes myogenesis by protecting *IGF2* transcripts from miR-125b-mediated suppression.[31] Another, lncRNA, *FER1L4*, play important roles in post-transcriptional regulation in gastric cancer by competing for shared miR-106a-5p.[32] In addition, a circular RNA that contains about 70 MREs with miR-7 was identified.[33] The circular RNA function as efficient miRNA sponge to sequesters miR-7 away from its targets and suppresses its function.

Many studies suggest the important role of lncRNAs in skeletal muscle myogenesis while highlighting the necessity to systematically identify lncRNAs altered in skeletal muscle development. In this study, we constructed the ceRNA network jointed by lncRNAs, miRNAs, and mRNAs. MiR-15a, miR-15b-5p, and miR-15b-5p are the core of this network, and they commonly target with *IRS1* which is the key signal transduction gene of IGF-1 signalling pathway. In addition,

we identify a skeletal muscle-enriched *lncIRS1* that promotes myogenesis *in vitro*. In the initial stage of skeletal muscle development, muscle precursor cells differentiate from the somite.[4] In this study, we identified that *IRS1* and *lncIRS1* were abundantly expressed in somite. During myoblasts proliferation and differentiation, the expression level of *IRS1* and *lncIRS1* are gradually increased, while the opposite expression pattern of miR-15a, miR-15b-5p, and miR-15c-5p were observed. Overexpression of those miRNAs simultaneously decreased the expression level of *IRS1* and *lncIRS1*. By functioning as a ceRNA, *lncIRS1* bocks miR-15a, miR-15b-5p, and miR-15c-5p to control the abundance of IRS1 protein and phosphorylation level of AKT. *IRS1* is downstream of the *IGF-1* receptor and is well known to be principal substrate for *IGF-1*, which mediated the IGF1-PI3K/AKT signalling pathway.[7] In mice, knockout of *IRS1* down-regulated the expression of *IGF-1* and led to 40–70% weight loss.[5,6]

Muscle atrophy is due to a decrease in muscle mass and fibre size. White muscle fibre atrophy occurs under conditions of tough nutritional restriction.[34] In mammals, inactivity and starvation lead to skeletal muscle atrophy.[35] Muscle atrophy also results from a co-morbidity of some common diseases, such as AIDS, congestive heart failure, cancer, chronic obstructive pulmonary disease, renal failure, and severe burns. *Atrogin-1* and *MuRF1* expressions correlated with loss of muscle protein.[36] In our study, *lncIRS1* controls the expression of *Atrogin-1* and *MuRF1* genes. It has been reported that dexamethasone can increase atrophy-related gene expressions in myotubes, while IGF-I inhibits their expression and blocks dexamethasone effects.[26] The converse of atrophy is hypertrophy, which is induced by an increase in protein synthesis and is characterized by an increase in muscle fibre size. In contrast to atrophy, however, high-rigour marker genes of the hypertrophy condition have not been well validated. Skeletal muscle hypertrophy is accompanied by the increased expression of IGF-1.[37] AKT is a central component in IGF1-PI3K/AKT pathway; it controls not only protein synthesis via the kinases mammalian target of rapamycin and glycogen synthase kinase 3β but also protein degradation via the FOXO family transcription factor. In this study, we used myoblast models of hypertrophy for studying the underlying mechanisms that regulate skeletal muscle hypertrophy. Recent studies have shown that the hypertrophy-inducing IGF-1-PI3K/AKT pathway could dominantly block the atrophy-inducing effects of dexamethasone, via AKT mediated phosphorylation and subsequent inhibition of the FOXO family of transcription factors.[38,39] In this study, we identified that *lncIRS1* can activate IGF1-PI3K/AKT pathway by acting as a sponge for miR-15 family to relieve *IRS1* expression (Figure 9L). Overexpression of *lncIRS1* promotes the expression of IGF-1, activates AKT phosphorylation, and increases skeletal muscle proliferation and total myotube numbers. From a clinical perspective, *lncIRS1* can promote the expression of IGF-1 and modulate key atrophy induced genes, such as *Atrogin-1* and *MuRF1* via the PI3K/AKT pathway, which may be used as a therapeutic target for muscle atrophy.

It has been reported that lncRNA *MAR1* played a positive role in skeletal muscle differentiation and growth *in vitro* and *in vivo*.[40] To test the function of the *lncIRS1 in vivo*, we performed *lncIRS1* overexpression or knockdown by direct injection of lentiviral particles in breast muscle. In our study, direct injection of overexpression of *lncIRS1* lentiviral particles into the breast muscle weakened the muscle atrophy, evidenced by the enhanced breast muscle weight, higher muscle fibre fusion index and higher myogenic marker (*MyoG* and *MyHC*) protein expression levels than did the negative control group. However, in the lentiviral-*lncIRS1* knockdown experiment, the opposite was true. These results show the therapeutic potential of *lncIRS1* in muscle atrophy.

In conclusion, we identified a novel *lncIRS1* acts as a sponge for miR-15 family to activate IGF1-PI3K/AKT signalling, resulting in promoting muscle proliferation, differentiation, and muscle mass, which may be used as a potential therapeutic agent for treating muscle atrophy.

Acknowledgements

This work was supported by the Ten-Thousand Talents Program (W03020593), Natural Scientific Foundation of China (31761143014), the Chinese Postdoctoral Science Foundation (2017M622715), Natural Science Foundation of Guangdong Province (2018A030310209), the China Agriculture Research System (CARS-41-G03), and Open Fund of Guangdong Provincial Key Laboratory of Agro-animal Genomics and Molecular Breeding, South China Agricultural University.

The authors certify that they comply with the ethical guidelines for authorship and publishing of the Journal of Cachexia, Sarcopenia and Muscle.[41]

Online supplementary material

Additional supporting information may be found online in the Supporting Information section at the end of the article.

Table S1. Differential expression analysis of lncRNAs in breast muscle between hypertrophic and leaner broilers.
Table S2. Differential expression analysis of genes in breast muscle between hypertrophic and leaner broilers.
Table S3. Differential expression analysis of miRNAs in breast muscle between hypertrophic and leaner broilers.
Table S4. Differentially expressed miRNAs and theirs corresponding target genes with differential expression in hypertrophic and leaner broilers.
Table S5. Differentially expressed miRNAs and theirs corresponding target lncRNAs with differential expression in

hypertrophic and leaner broilers.

Table S6. Summary of the represented networks generated by IPA analysis.

Table S7. The full length sequences of *lncIRS1* and *IRS1*

Table S8. Information of Primers.

Fig S1 A competing endogenous RNA (ceRNA) hypothesis. LncRNAs and mRNAs, which share the common miRNA response elements (MREs), could influence each other's levels by competing for a limited pool of miRNA. **(a)** Upregulation of lncRNA increases cellular concentrations of particular MREs and can result in the derepression of mRNA that contains the same MREs. **(b)** While downregulation of lncRNA would lead to decreased levels of particular MREs, and, consequently inhibited the expression of mRNA.

Fig S2 miRNA-gene interaction network

Hypertrophic broiler vs. leaner broiler, differentially expressed miRNAs and their corresponding differentially expressed target genes with opposition expression pattern were used to construct a miRNA-gene interaction network. In this network, miRNAs are displayed as pink circles, and miRNA target genes are displayed as blue circles. Dashed lines represent the interactions between differentially expressed miRNAs and theirs corresponding target genes.

Fig S3 miRNA-lncRNA interaction network

Hypertrophic broiler vs. leaner broiler, differentially expressed miRNAs and their corresponding differentially expressed target lncRNAs with opposition expression pattern were used to construct a miRNA-lncRNA interaction network. In this network, miRNAs are displayed as pink circles, and miRNA target lncRNAs are displayed as green circles. Solid lines represent the interactions between differentially expressed miRNAs and theirs corresponding target lncRNAs.

Fig S4 Ingenuity Pathway Analysis (IPA) identification of gene networks

IPA online software was used to identify the gene-gene interaction networks, using the genes in the miRNA-gene network as input. (**a-d**) A total of four major gene networks were identified. Nodes shaded in blue represent the genes from miRNA-gene network are also involved in the IPA interaction network. White nodes represent transcription factors (as opposed to gene from miRNA-gene network) that are associated with the regulation of some of these genes, based on the evidence stored in the IPA knowledgebase. Edges and node are annotated with labels that illustrate the nature of the relationship between the genes and their functions.

Fig S5 GO and pathway analysis of the gene from lncRNA-miRNA-gene network(**a**)

The top 10 enriched terms for three GO categories (biological process, cellular component and molecular function) for the genes belonging to lncRNA-miRNA-gene network. (**b**) The top 10 enriched pathway for the genes belonging to lncRNA-miRNA-gene network. Pink bars represent the pathway associated with muscle growth. (**c**) The network between genes and theirs associated pathway. Yellow oval represent the genes that from lncRNA-miRNA-gene network, while blur bar represent these pathway that they enrich in. (**d**) Pathway analysis indicates that the genes (*IRS1*) from lncRNA-miRNA-gene are enriched in the IGF-1 signaling pathway. *IRS1* (nodes shaded) function in the IGF-1 signaling pathway.

Fig S6 *LncIRS1* acts as a sponge of miR-15a, miR-15b-5p and miR-15c-5p to regulate the expression of *IRS1*

MiR-15a, miR-15b-5p and miR-15c-5p inhibit the RNA expression level of lncIRS1 **(a)**, and simultaneously depress the expression of *IRS1* **(b)**. **(c)** Co-expression of miR-15a, miR-15b-5p or miR-15c-5p, and lncIRS1 upregulate the RNA expression level of *IRS1*.

Conflict of interest

Z.L., B.C., B.A.A., X.Z., M.Z., P.H., Q.N., and X.Z. declare that they have no conflict of interest.

References

1. Jagoe RT, Goldberg AL. What do we really know about the ubiquitin-proteasome pathway in muscle atrophy? *Curr Opin Clin Nutr Metab Care* 2001;**4**:183–190.
2. Hasselgren PO. Glucocorticoids and muscle catabolism. *Curr Opin Clin Nutr Metab Care* 1999;**2**:201–205.
3. Goldspink DF, Garlick PJ, McNurlan MA. Protein turnover measured in vivo and in vitro in muscles undergoing compensatory growth and subsequent denervation atrophy. *Biochem J* 1983;**210**:89–98.
4. Li Z, Ouyang H, Zheng M, Cai B, Han P, Abdalla BA, et al. Integrated analysis of long non-coding RNAs (LncRNAs) and mRNA expression profiles reveals the potential role of LncRNAs in skeletal muscle development of the chicken. *Front Physiol* 2016;**7**:687.
5. Dong X, Park S, Lin X, Copps K, Yi X, White MF. Irs1 and Irs2 signaling is essential for hepatic glucose homeostasis and systemic growth. *J Clin Invest* 2006;**116**:101–114.
6. Tamemoto H, Kadowaki T, Tobe K, Yagi T, Sakura H, Hayakawa T, et al. Insulin resistance and growth retardation in mice lacking insulin receptor substrate-1. *Nature* 1994;**372**:182–186.
7. Schiaffino S, Mammucari C. Regulation of skeletal muscle growth by the IGF1-Akt/PKB pathway: insights from genetic models. *Skelet Muscle* 2011;**1**:4.
8. Morris KV, Mattick JS. The rise of regulatory RNA. *Nat Rev Genet* 2014;**15**:423–437.

9. Guttman M, Rinn JL. Modular regulatory principles of large non-coding RNAs. *Nature* 2012;**482**:339–346.
10. Fatica A, Bozzoni I. Long non-coding RNAs: new players in cell differentiation and development. *Nat Rev Genet* 2014;**15**:7–21.
11. Caretti G, Schiltz RL, Dilworth FJ, Di Padova M, Zhao P, Ogryzko V, et al. The RNA helicases p68/p72 and the noncoding RNA SRA are coregulators of MyoD and skeletal muscle differentiation. *Dev Cell* 2006;**11**: 547–560.
12. Salmena L, Poliseno L, Tay Y, Kats L, Pandolfi PP. A ceRNA hypothesis: the Rosetta Stone of a hidden RNA language? *Cell* 2011;**146**:353–358.
13. Ebert MS, Neilson JR, Sharp PA. MicroRNA sponges: competitive inhibitors of small RNAs in mammalian cells. *Nat Methods* 2007;**4**:721–726.
14. Poliseno L, Salmena L, Zhang J, Carver B, Haveman WJ, Pandolfi PP. A coding-independent function of gene and pseudogene mRNAs regulates tumour biology. *Nature* 2010;**465**:1033–1038.
15. Cesana M, Cacchiarelli D, Legnini I, Santini T, Sthandier O, Chinappi M, et al. A long noncoding RNA controls muscle differentiation by functioning as a competing endogenous RNA. *Cell* 2011;**147**:358–369.
16. Kallen AN, Zhou XB, Xu J, Qiao C, Ma J, Yan L, et al. The imprinted H19 lncRNA antagonizes let-7 microRNAs. *Mol Cell* 2013;**52**: 101–112.
17. Henrique D, Adam J, Myat A, Chitnis A, Lewis J, Ish-Horowicz D. Expression of a Delta homologue in prospective neurons in the chick. *Nature* 1995;**375**:787–790.
18. Luo W, Wu H, Ye Y, Li Z, Hao S, Kong L, et al. The transient expression of miR-203 and its inhibiting effects on skeletal muscle cell proliferation and differentiation. *Cell Death Dis* 2014;**5**:e1347.
19. Livak KJ, Schmittgen TD. Analysis of relative gene expression data using real-time quantitative PCR and the 2(-Delta Delta C(T)) method. *Methods* 2001;**25**:402–408.
20. Luo W, Chen J, Li L, Ren X, Cheng T, Lu S, et al. c-Myc inhibits myoblast differentiation and promotes myoblast proliferation and muscle fibre hypertrophy by regulating the expression of its target genes, miRNAs and lincRNAs. *Cell Death Differ* 2018; https://doi.org/10.1038/s41418-018-0129-0.
21. Ouyang H, He X, Li G, Xu H, Jia X, Nie Q, et al. Deep sequencing analysis of miRNA expression in breast muscle of fast-growing and slow-growing broilers. *Int J Mol Sci* 2015;**16**:16242–16262.
22. Baker J, Liu JP, Robertson EJ, Efstratiadis A. Role of insulin-like growth factors in embryonic and postnatal growth. *Cell* 1993;**75**:73–82.
23. Araki E, Lipes MA, Patti ME, Bruning JC, Haag BR, Johnson RS, et al. Alternative pathway of insulin signalling in mice with targeted disruption of the IRS-1 gene. *Nature* 1994;**372**:186–190.
24. Kong L, Zhang Y, Ye ZQ, Liu XQ, Zhao SQ, Wei L, et al. CPC: assess the protein-coding potential of transcripts using sequence features and support vector machine. *Nucleic Acids Res* 2007;**35**: W345–W349.
25. Luo W, Nie Q, Zhang X. MicroRNAs involved in skeletal muscle differentiation. *J Genet Genomics* 2013;**40**:107–116.
26. Bodine SC, Latres E, Baumhueter S, Lai VK, Nunez L, Clarke BA, et al. Identification of ubiquitin ligases required for skeletal muscle atrophy. *Science* 2001;**294**:1704–1708.
27. Wang L, Luo GJ, Wang JJ, Hasselgren PO. Dexamethasone stimulates proteasome- and calcium-dependent proteolysis in cultured L6 myotubes. *Shock* 1998;**10**: 298–306.
28. Levine S, Biswas C, Dierov J, Barsotti R, Shrager JB, Nguyen T, et al. (2011) Increased proteolysis, myosin depletion, and atrophic AKT-FOXO signaling in human diaphragm disuse. *Am J Respir Crit Care Med* 2011;**183**:483–490.
29. Ebert MS, Sharp PA. Emerging roles for natural microRNA sponges. *Curr Biol* 2010;**20**:R858–R861.
30. Karreth FA, Pandolfi PP. ceRNA cross-talk in cancer: when ce-bling rivalries go awry. *Cancer Discov* 2013;**3**:1113–1121.
31. Zhu M, Liu J, Xiao J, Yang L, Cai M, Shen H, et al. Lnc-mg is a long non-coding RNA that promotes myogenesis. *Nat Commun* 2017;**8**:14718.
32. Xia T, Liao Q, Jiang X, Shao Y, Xiao B, Xi Y, et al. Long noncoding RNA associated-competing endogenous RNAs in gastric cancer. *Sci Rep* 2014;**4**:6088.
33. Memczak S, Jens M, Elefsinioti A, Torti F, Krueger J, Rybak A, et al. Circular RNAs are a large class of animal RNAs with regulatory potency. *Nature* 2013;**495**:333–338.
34. Maddock DM, Burton MP. Some effects of starvation on the lipid and skeletal muscle layers of the winter flounder, *Pleuronectes americanus*. *Can J Zool* 1994;**72**: 1672–1679.
35. Fuster G, Busquets S, Almendro V, López-Soriano FJ, Argilés JM. Antiproteolytic effects of plasma from hibernating bears: a new approach for muscle wasting therapy? *Clin Nutr* 2007;**26**:658–661.
36. Sacheck JM, Ohtsuka A, McLary SC, Goldberg AL. IGF-I stimulates muscle growth by suppressing protein breakdown and expression of atrophy-related ubiquitin ligases, Atrogin-1 and MuRF1. *Am J Physiol Endocrinol Metab* 2004;**287**:E591–E601.
37. DeVol DL, Rotwein P, Sadow JL, Novakofski J, Bechtel PJ. Activation of insulin-like growth factor gene expression during work-induced skeletal muscle growth. *Am J Physiol* 1990;**259**:E89–E95.
38. Sandri M, Sandri C, Gilbert A, Skurk C, Calabria E, Picard A, et al. Foxo transcription factors induce the atrophy-related ubiquitin ligase Atrogin-1 and cause skeletal muscle atrophy. *Cell* 2004;**117**:399–412.
39. Stitt TN, Drujan D, Clarke BA, Panaro F, Timofeyva Y, Kline WO, et al. The IGF-1/PI3K/Akt pathway prevents expression of muscle atrophy-induced ubiquitin ligases by inhibiting FOXO transcription factors. *Mol Cell* 2004;**14**:395–403.
40. Zhang ZK, Li J, Guan D, Liang C, Zhuo Z, Liu J, et al. A newly identified lncRNA MAR1 acts as a miR-487b sponge to promote skeletal muscle differentiation and regeneration. *J Cachexia Sarcopenia Muscle* 2018;**9**:613–626.
41. von Haehling S, Morley JE, Coats AJS, Anker SD. Ethical guidelines for publishing in the Journal of Cachexia, Sarcopenia and Muscle: update 2017. *J Cachexia Sarcopenia Muscle* 2017;**8**:1081–1083.